ChEESE

Center of Excellence for Exascale in Solid Earth

WP4-PD1

Urgent seismic simulations

Fast statistical determination of focal mechanisms

Marisol Monterrubio-Velasco, Otilio Rojas, Juan Rodríguez and Josep de la Puente.

Questions: It is possible to determine the CMT of a new event using a “close” historical one? Which is the uncertainty of this method?

1. Introduction

The analysis of focal mechanisms provide information on the fault plane of earthquakes, and on the directions of the principal stresses in the areas where earthquake occur (Maeda, 1992). One of the key parameter in the Urgent seismic computing (PD1) workflow, is the real time computation of focal mechanism. The most general approach for determine this information is the computation of the moment tensor, which provides unique and robust information regarding the fault-plane orientations and the size of the event. For moderate-to-large earthquakes, the moment tensor is usually obtained from the full waveforms modeling of far-field seismic records or spectral data inversions (Tarantino et al., 2019, and references therein). The rapid determination of earthquake magnitude and focal mechanism, important for a number of rapid response applications including tsunami warning, is still challenging because of the limitations of near-field inertial recordings (Jiun-Ting et al., 2019). Although the approaches for estimating earthquake location and magnitude are now consolidated, automatic solutions for the focal mechanism are not always provided by the agencies or available at later times after inversion of waveforms for the determination of moment tensor components (Tarantino et al., 2019).
Some significant efforts has been done to determine in a real-time the focal mechanism or centroid moment tensors using different methods and algorithms. For example, using GPS networks (Jiun-Ting et al., 2019; Melgar et al., 2012); a source inversion algorithm based on modelling of the W phase, a very long period phase (100-1000s) arriving at the same time as the P-wave (Duputel et al. 2012); or also azimuthal distribution of early P-wave peak in displacement, velocity and acceleration (Tarantino et al., 2019).
In this work, we explore the statistical capability of compare past events, in the determination of the focal mechanism for a new large-magnitude event. Therefore, we offer a tool to quantify the uncertainty in this kind of approaches. In order to reach these objectives, we test the statistical tool using different seismic active regions Japan, Southern California, Iceland and New Zealand.

2. Methodology

In this section, we describe the procedure followed in this work to propose a focal mechanism in a quick elapsed time.

1. Databases

The first step is the obtaintion of the historical CMT provided by https://ds.iris.edu/spud/momenttensor, which provide the information of past earthquakes including the CMT and the focal mechanism since 1950 in some cases.

2. Code development

We developed a python code to analyze the focal mechanisms and compare it with historical events. This code uses four main packages: Obspy, Numpy, Matplolib, and Basemap.
The first step in the numerical analysis is an statistical exploratory study to know the statistical distribution of our database. The second step is the methodology validation together with a quantification of the favorable cases where the focal mechanism of a "new" event is similar to some other historical earthquake. Therefore, to realize this second step, we consider the whole database and compare each event looking the "closer" event (s) from the database, first (k=1), second (k=2), third (k=3), and fourth (k=4) event. Moreover, we include in the comparison a hypothetical event which is build from the median measure for the strike, dip and rake, considering a k-nearest neighbors.
To compute how spatially close is one earthquake to another we use the Euclidean distance equation considering the Earth curvature in the epicentral distance by means the Heavisine formula (Sinnott, 1984)
To analyze the similitude between different focal mechanisms, the code includes the Minimum Rotated Angle, MRA, measures proposed in Kagan (2007). The MRA quantify the similarity in degrees between different focal mechanisms.
In our code we include a threshold magnitude parameter to analyze the events that are closer in space but also similar in magnitude. Is worth to mention that Okuda and Ide (2018) show that the initial seismic waveform and the focal mechanism of earthquakes that occur in the same region is independent of its magnitude. So, we also analyze the whole catalog without discriming by a threshold magnitude studying the Okuda and Ide (2018) assumption.
Therefore the procedure is: randomly choose events from the total database finding the most similar focal mechanism using the k-nearest neighbors. At the end we compute the number of favorable cases for which the methodology offers a close focal mechanism to the real one.

3. Results

Region name	Region latitude (minimum, maximum)	Region longitude (minimum, maximum)	max. depth (km)	Number of Events	(min., max. magnitude)	date (start, end)
Iceland	63.06, 66.94	-24.43 -16.58	33	124	4.6, 6.5	1976/01/13, 2018/12/28
Japan	30.03, 46.3	128.84, 147.1	588	2652	4.6, 9.1	1967/08/13, 2019/04/27
New Zealand	-46.02, -34.42	166.1 178.71	518	273	4.8, 7.8	1965/12/18, 2018/11/30
Italy	34.95, 47.94	5.18, 21.0	502	692	3.9, 6.9	1976/05/06, 2015/12/29
Southern	29.72	-129.76	30	460	4.4, 7.3	2010/10/24,

California	44.77	-110.36				2019/10/28

Table 1. THe five regions and its information used in this analysis.

3.1 Study case : Iceland

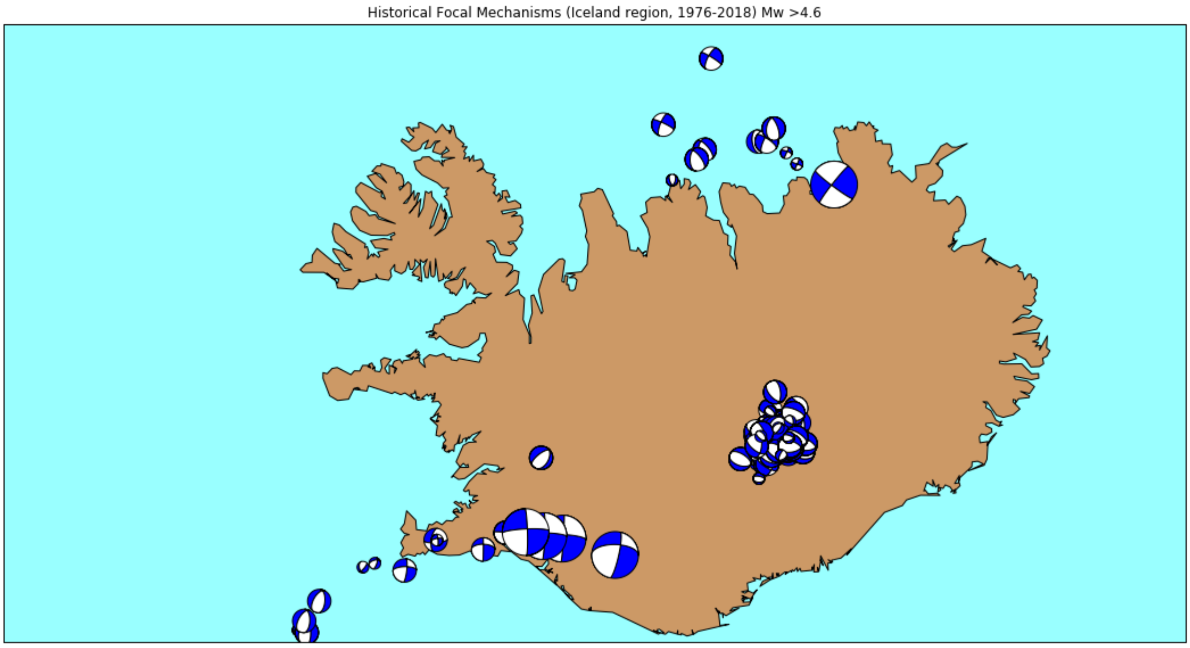

Fig. 1 Iceland region and the focal mechanisms database for M>4.6

Exploratory analysis

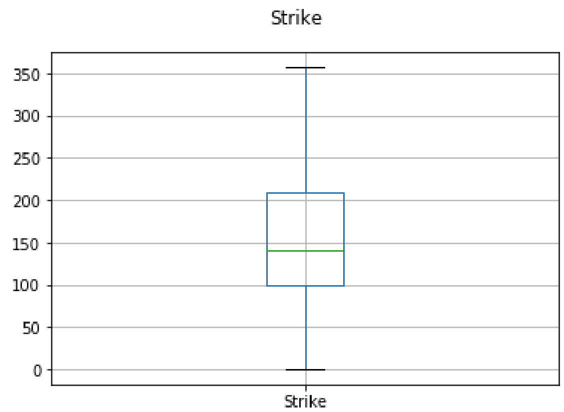

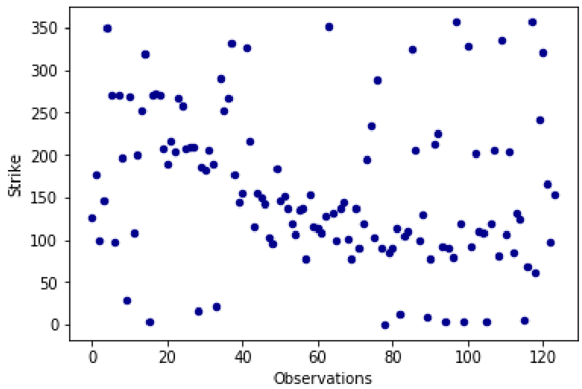

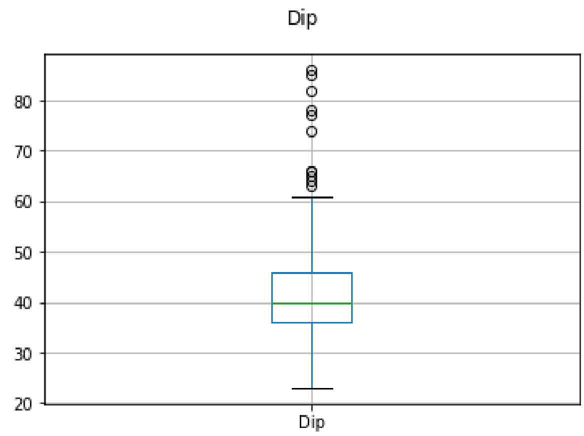

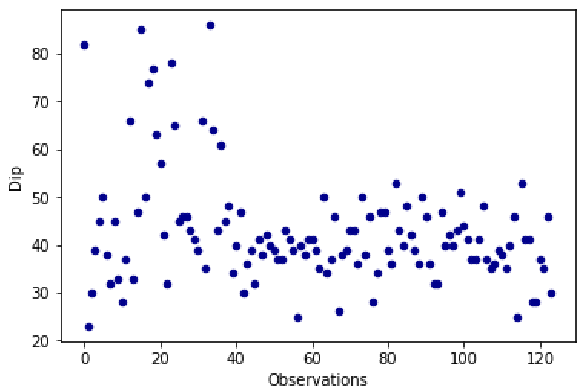

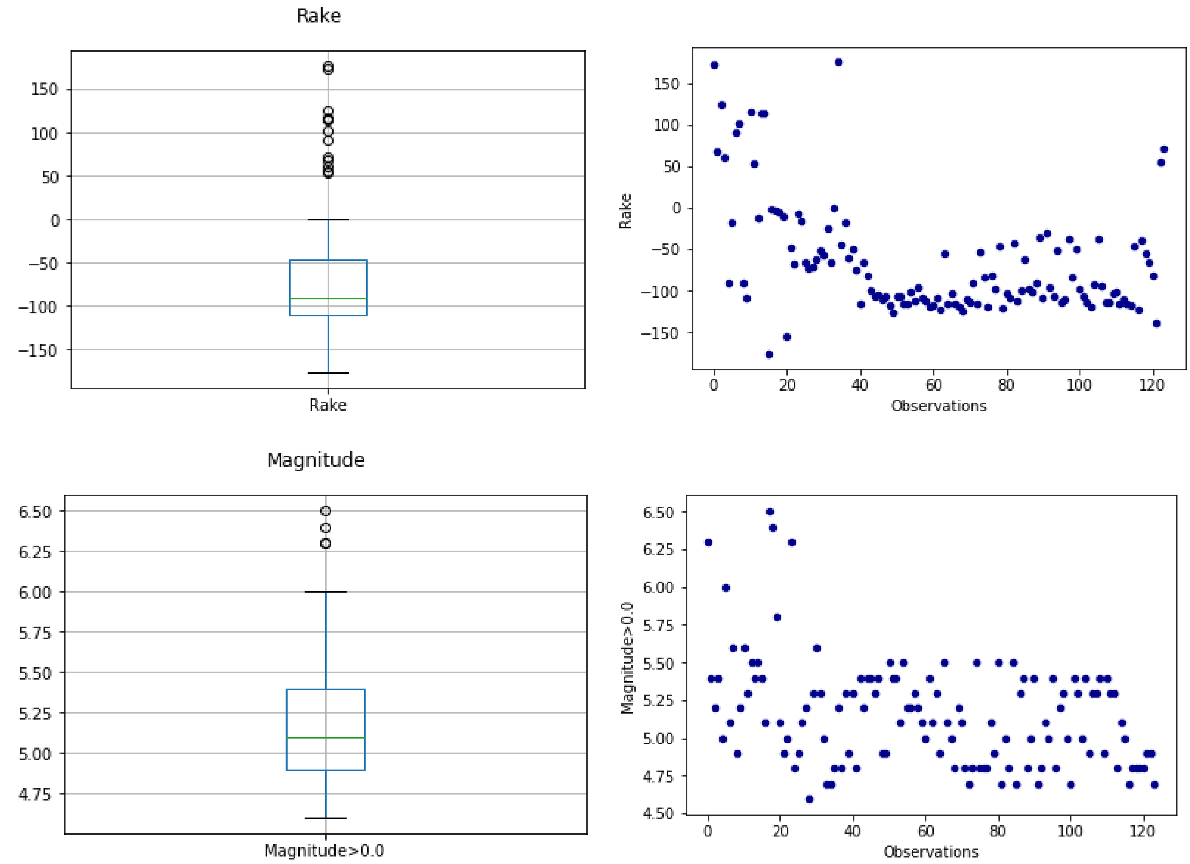

Fig. 2 Statistical distribution of strike, dip, rake and magnitude for Iceland database

Parameters

k = 20 # Number of neighbors
Dist_th = 30 # Maximum distance threshold [km]
Mag_th = 4.6 # Minimum magnitude threshold
Seed = 98

Minimum Rotated Angle Results

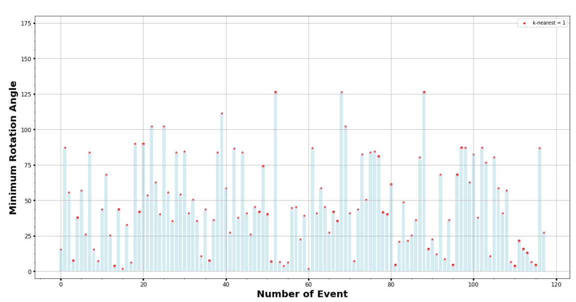

(a)

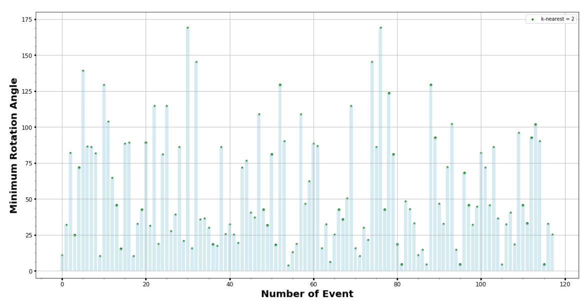

(b)

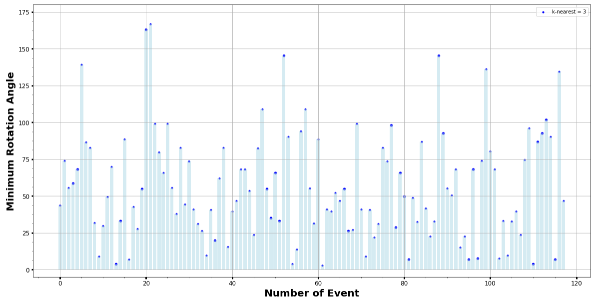

(c)

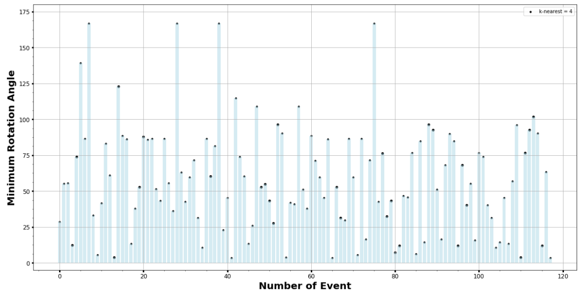

(d)

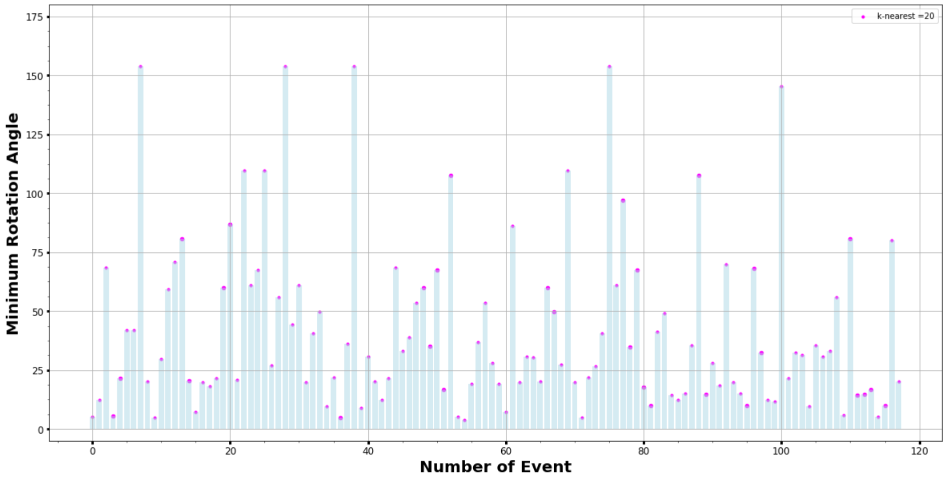

(e)

Fig. 3 Minimum rotated angle results for (a) k = 1 (closest neighbor in red), (b) k = 2 (second closest neighbor in blue), (c) k = 3 (third closest neighbor in green), (d) k = 4 (fourth closest neighbor in black) and (e) Hypothetical focal mechanism median values in strike, dip and rake (in magenta).

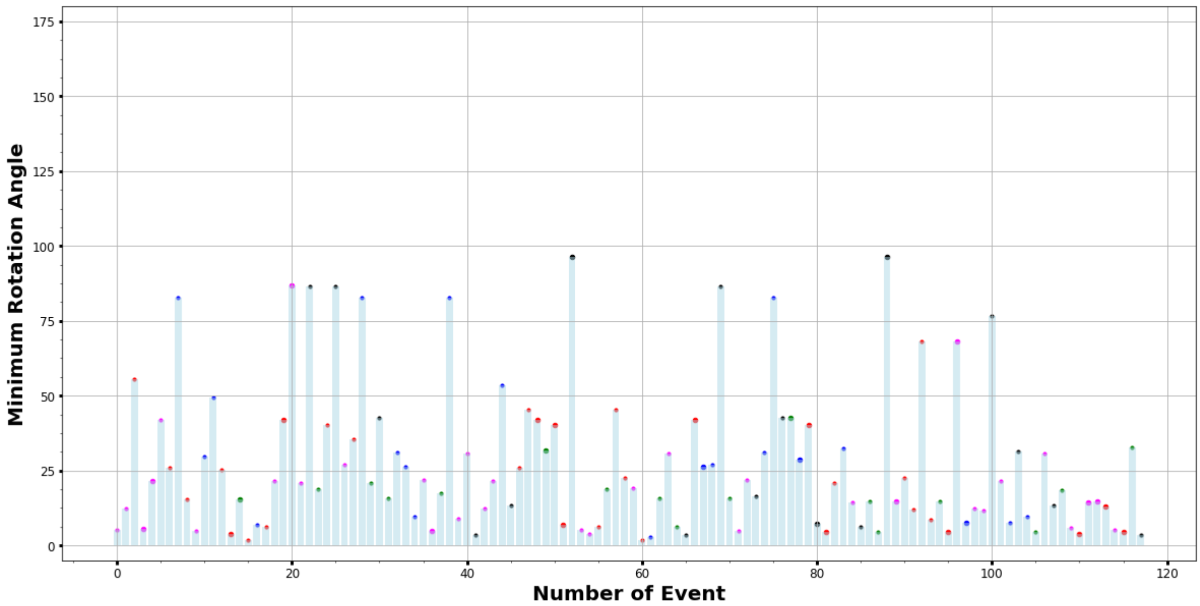

Fig. 4. Lower MRA values values that show the most similar focal mechanism for each case obtained from Fig. 3.

Example of the MRA and the resulted beach balls

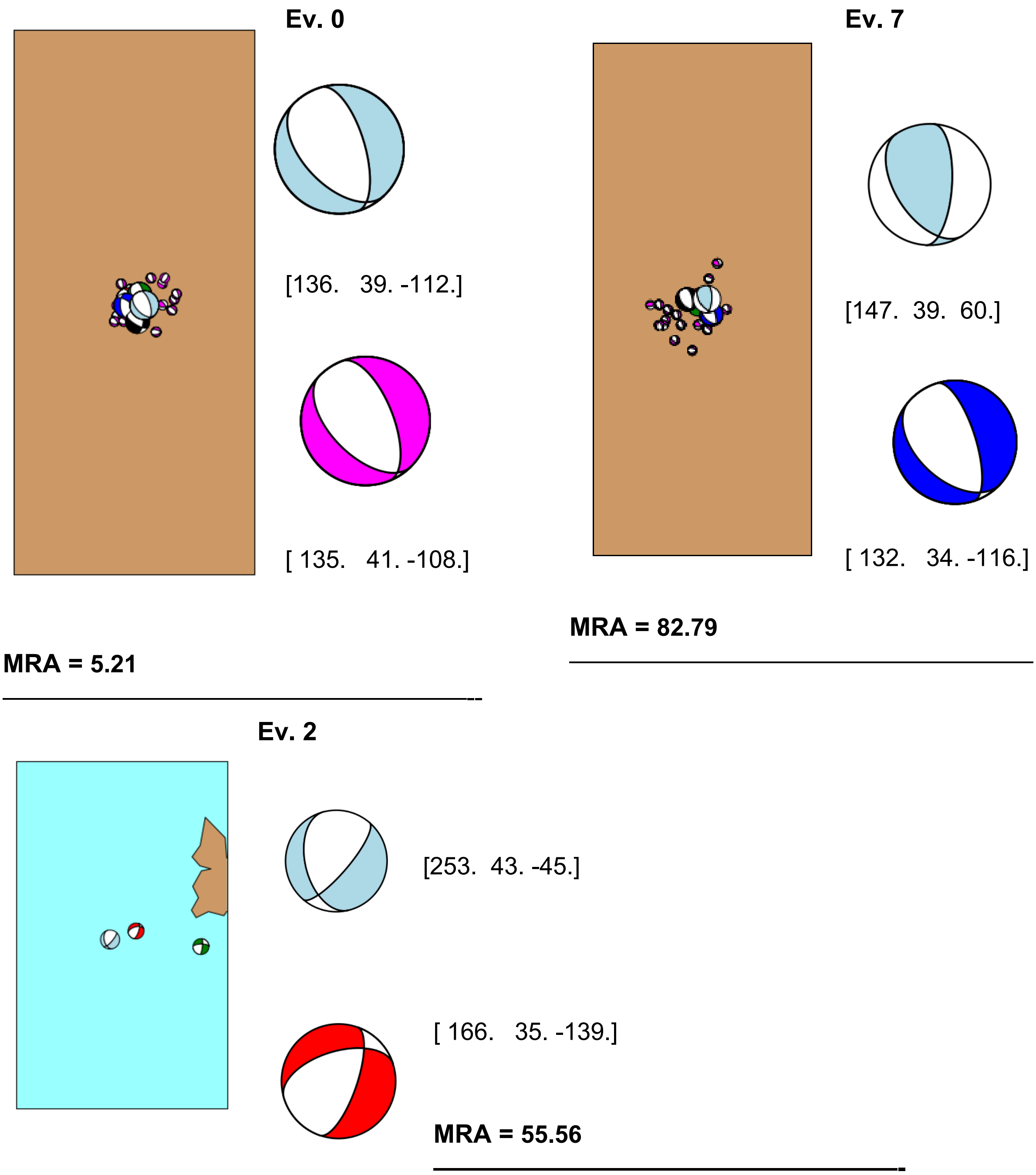

Fig. 5 Example of the MRA values and its relation with the beach balls and the focal mechanism values. The events correspond to Fig. 4 The colors of beach balls indicate:. light blue the "new event", red the closest event (k=1), blue for k = 2, green for k = 3, black for k = 4, and magenta for the hypothetical focal mechanism of median values in strike, dip and rake.

Results over random selection events: 124 in total

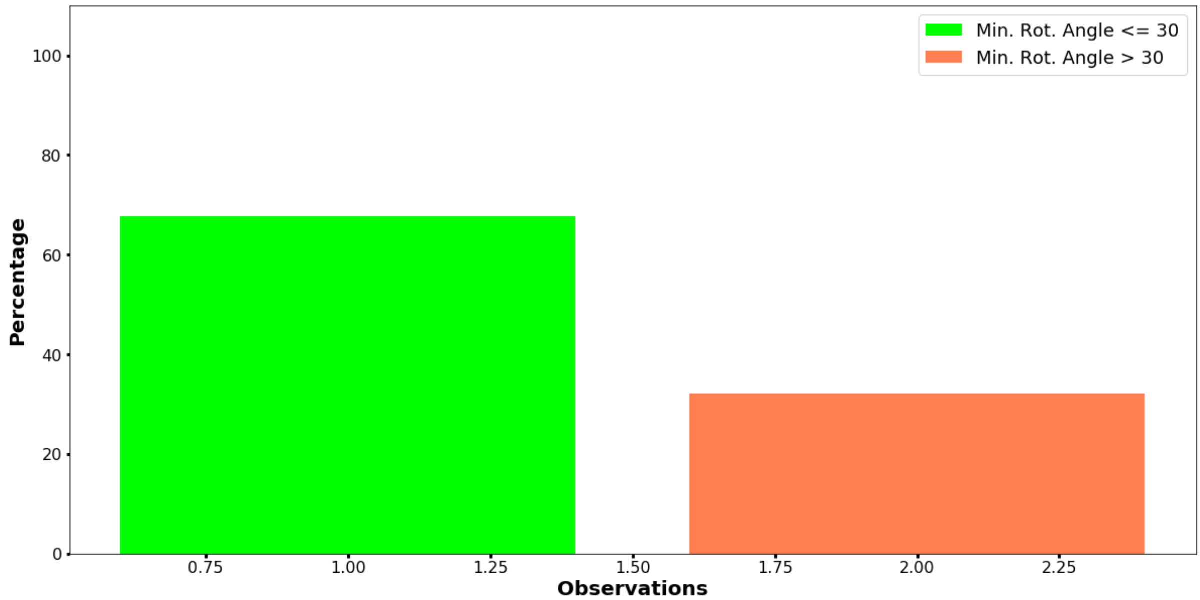

Fig. 6 Statistical results of MRA analysis. Percentage of similar focal mechanism shown in green, and non-similar focal mechanism in orange.

3.2 Study case : Japan

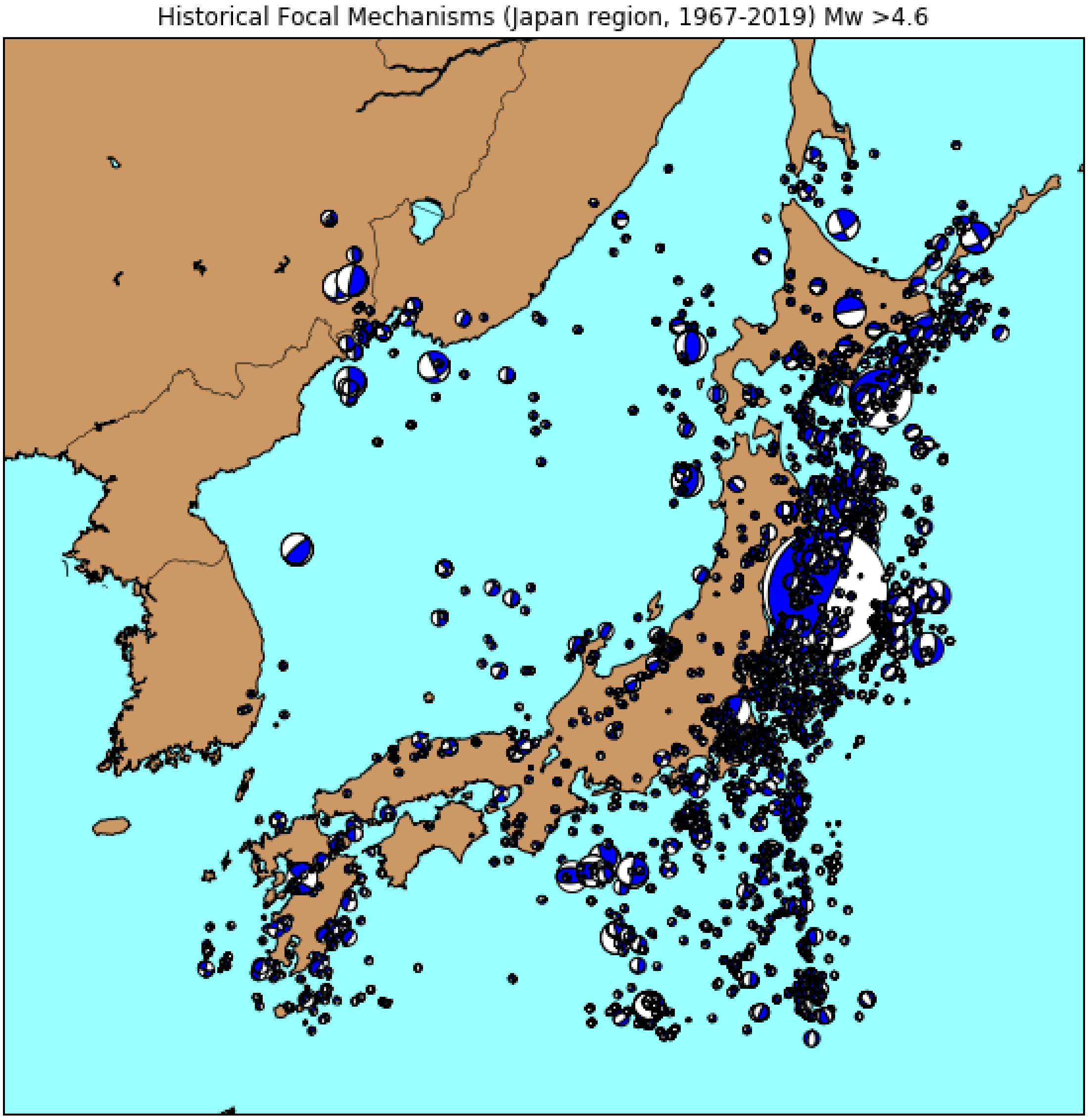

Fig. 7 Japan region and focal mechanisms database for M>4.6

Exploratory analysis

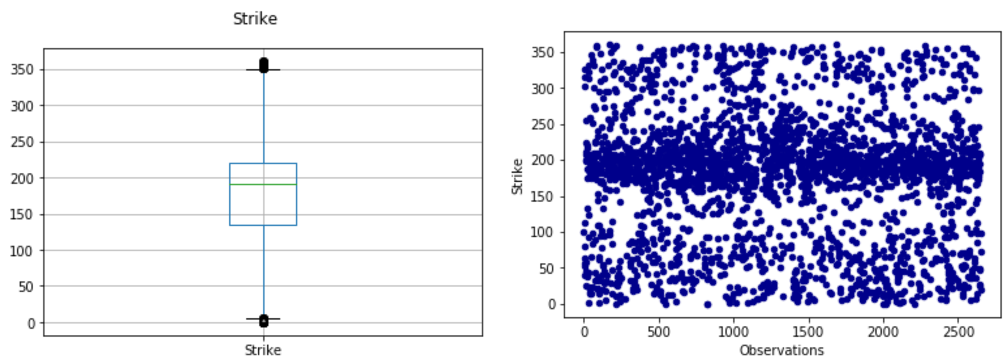

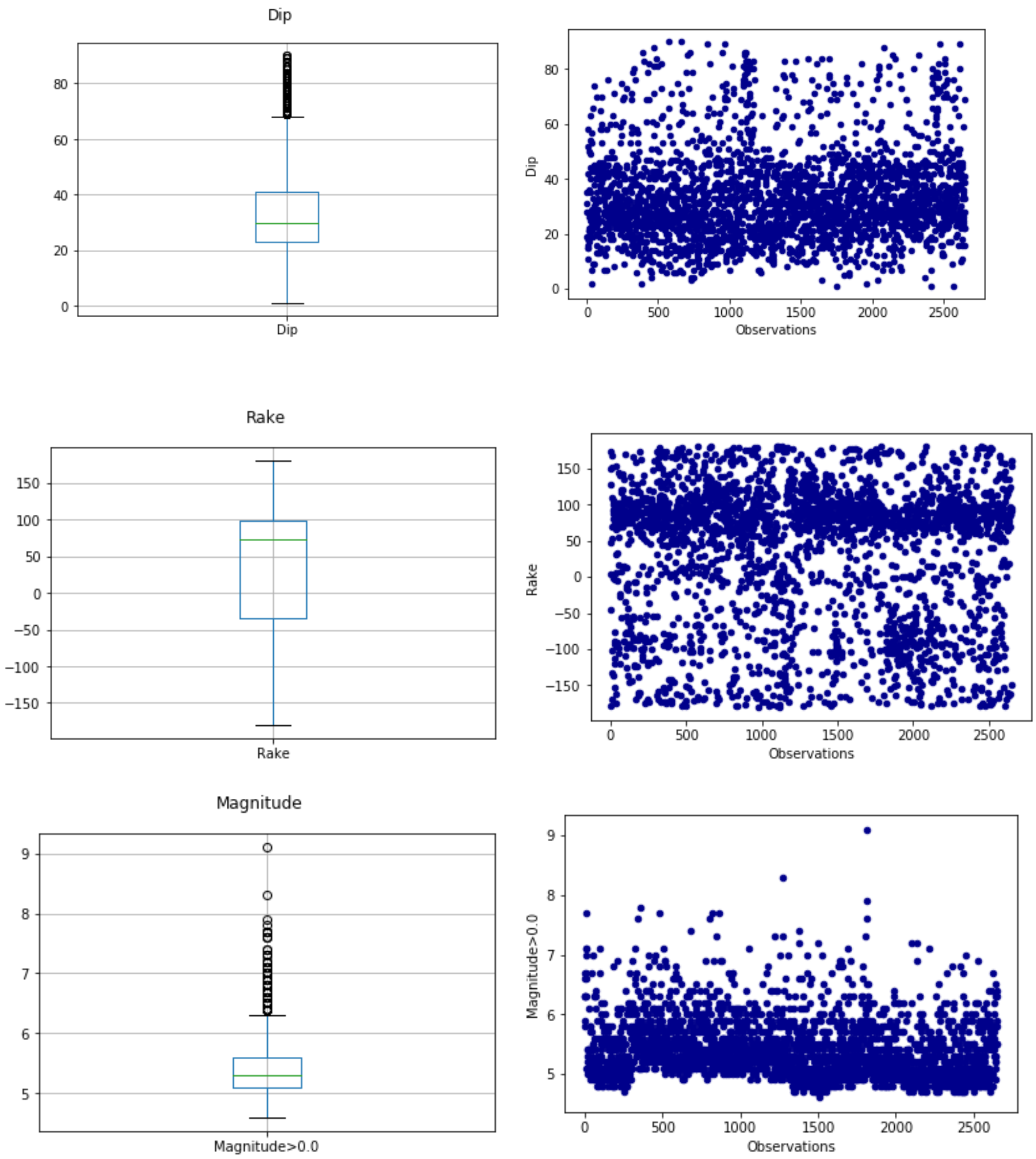

Fig. 8 Statistical distribution of strike, dip, rake and magnitude for Japan database

Parameters

k = 20 # Number of neighbors
Dist_th = 30 # Maximum distance threshold [km]
Mag_th = 5.5 # Minimum magnitude threshold
Seed = 98

Minimum Rotated Angle Results

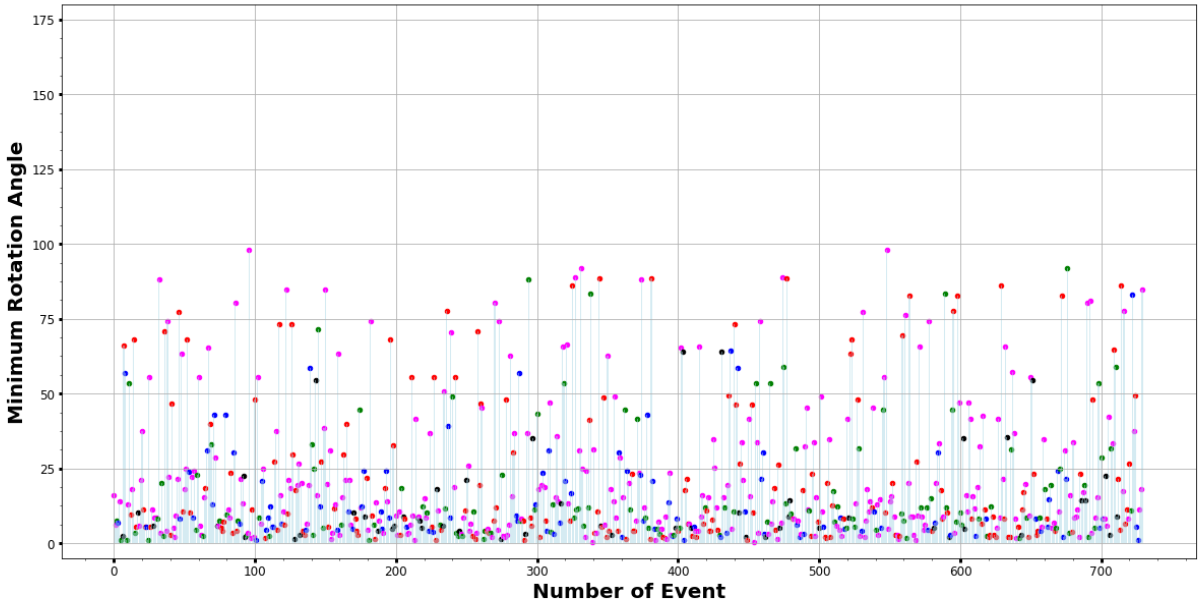

Fig. 9 MRA results combining the best values from k=1, 2, 3, 4 and the median hypothetical focal mechanism

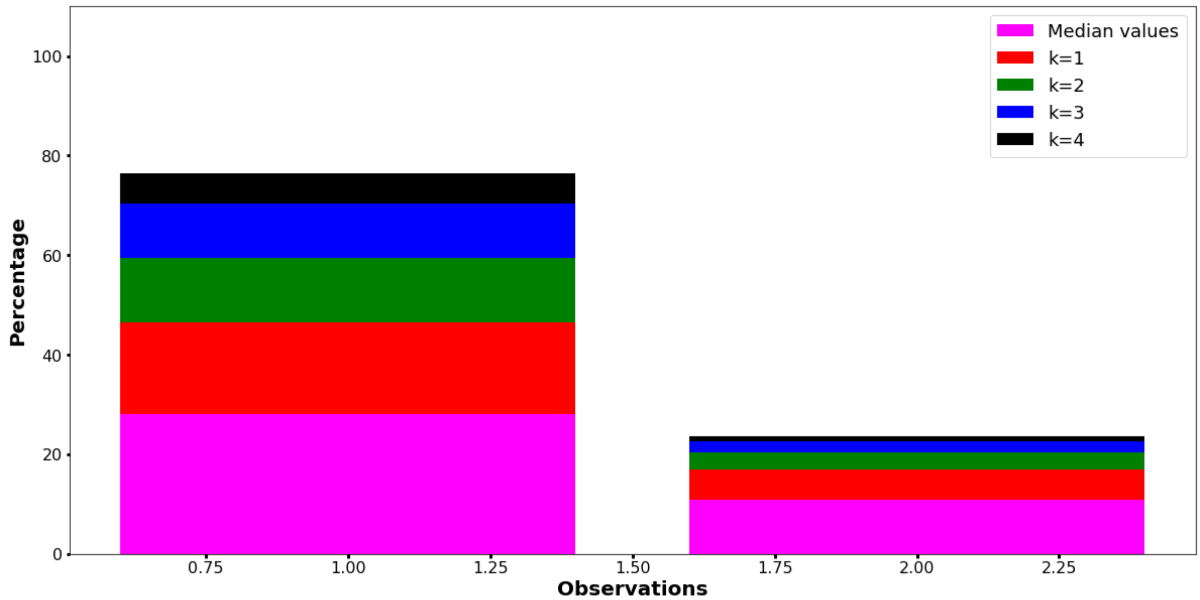

Results over random selection events: 750 approx.

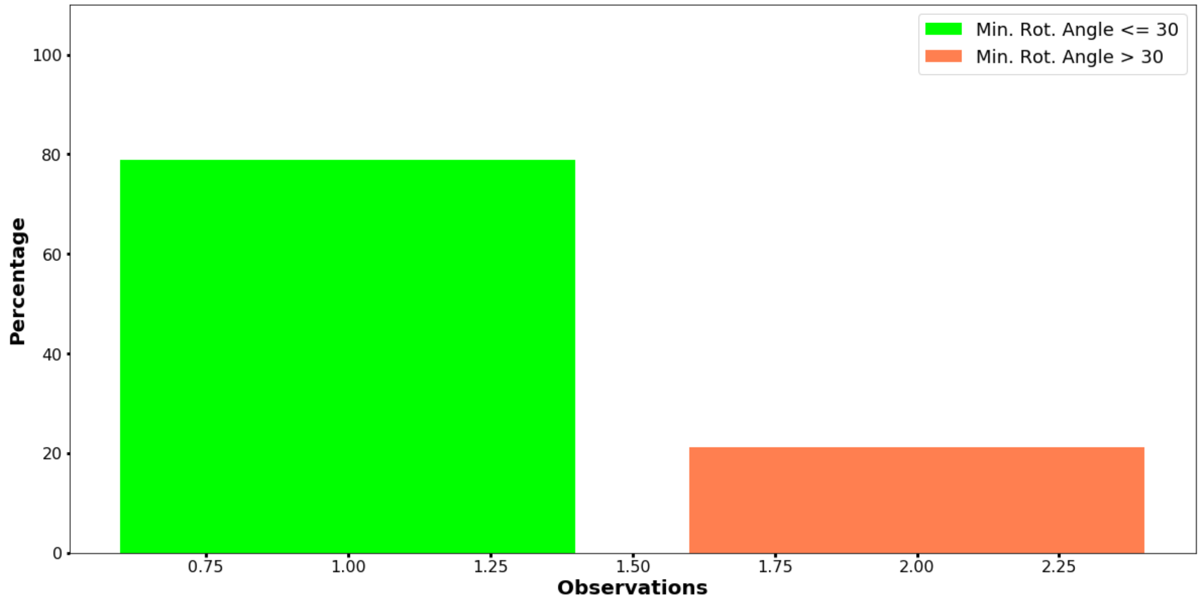

Fig. 10 Statistical results of MRA analysis. Percentage of similar focal mechanism shown in green, and non-similar focal mechanism in orange.

3.3 Study case : New Zealand (273 events)

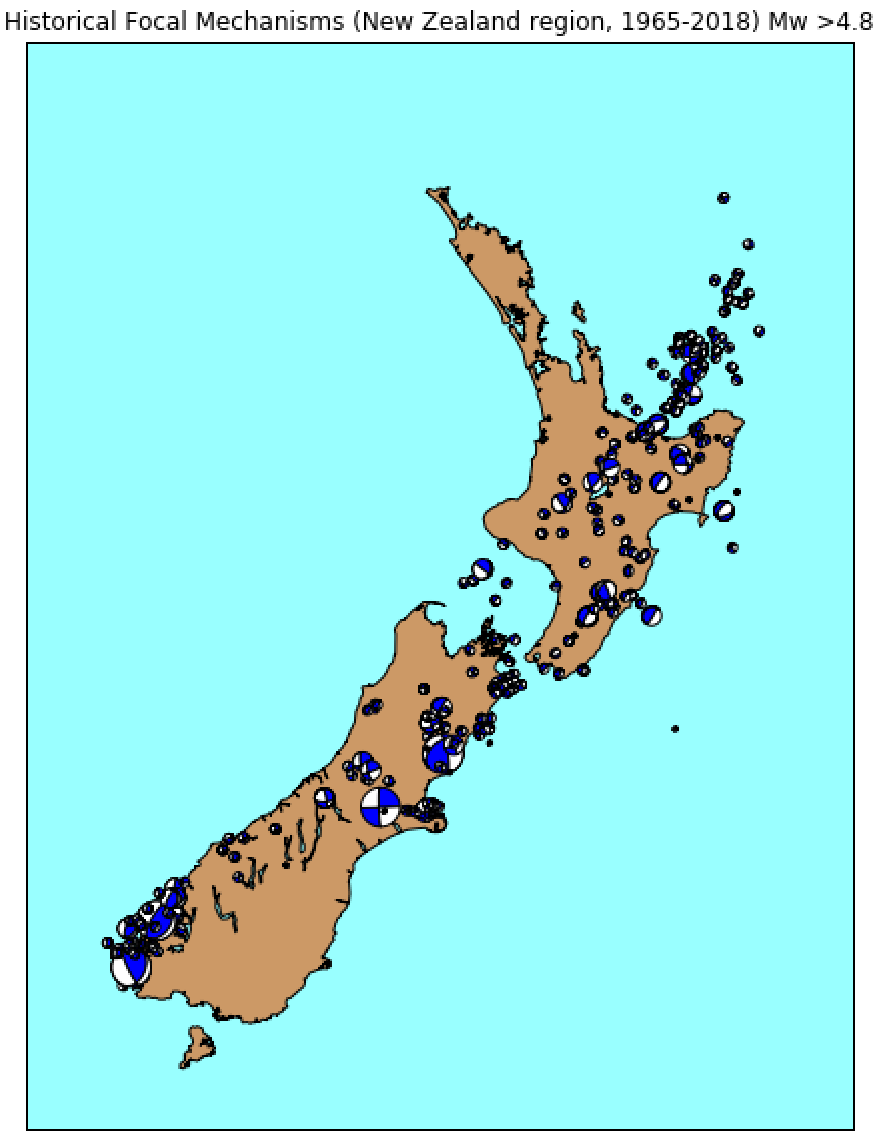

Fig. 11 New Zealand region and focal mechanisms database for M>4.8

Exploratory analysis

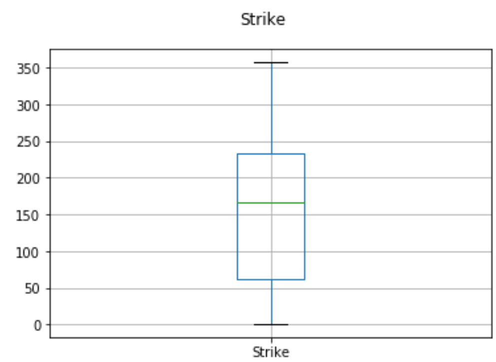

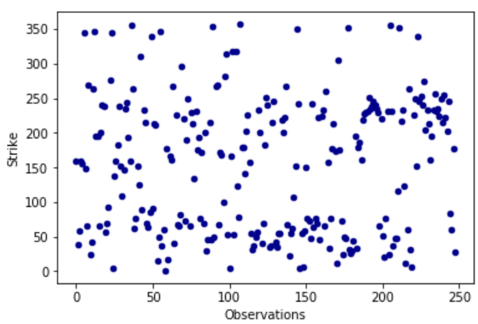

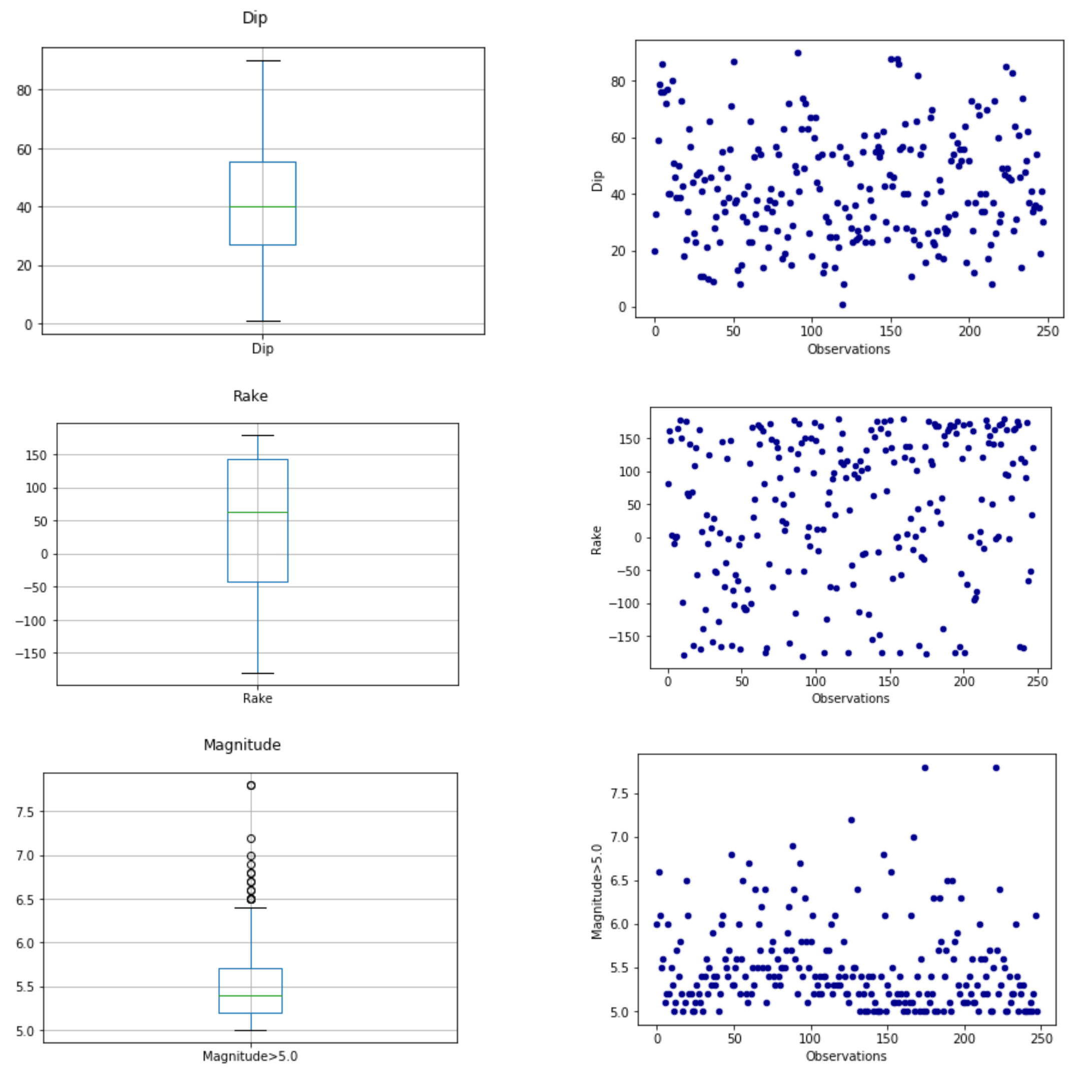

Fig. 12 Statistical distribution of strike, dip, rake and magnitude for Japan database

Parameters

k = 20 # Number of neighbors
Dist_th = 100 # Maximum distance threshold [km]
Mag_th = 4.8 # Minimum magnitude threshold
Seed = 98

Minimum Rotated Angle Results

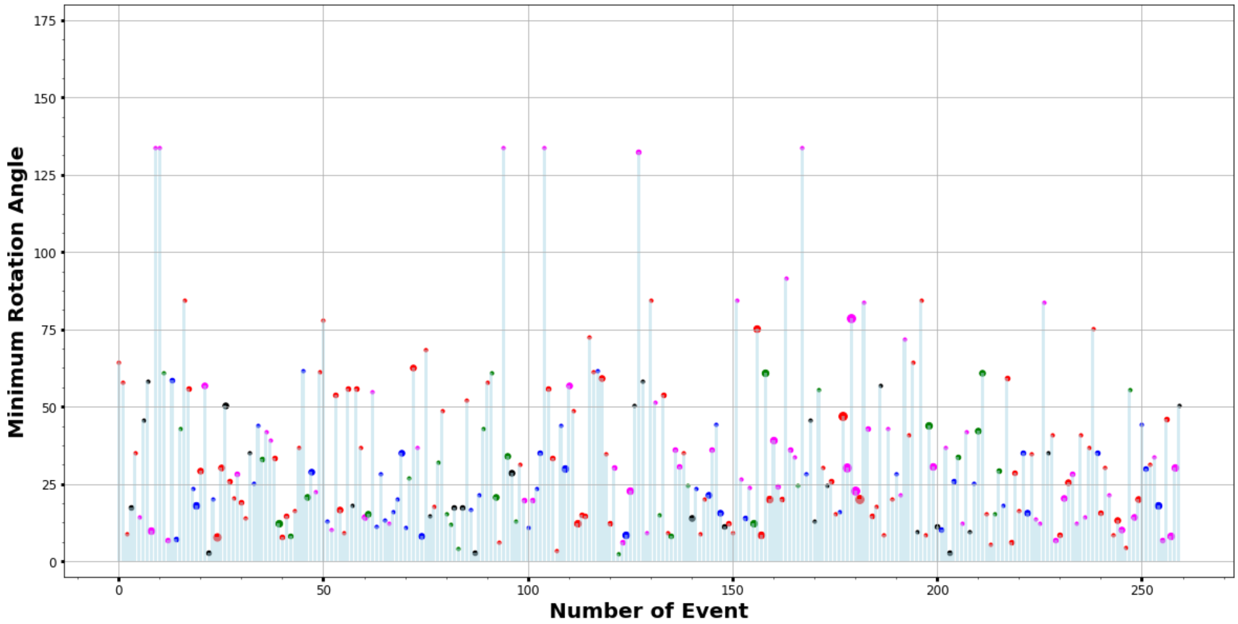

Fig. 13 MRA results combining the best values from k=1, 2, 3, 4 and the median hypothetical focal mechanism

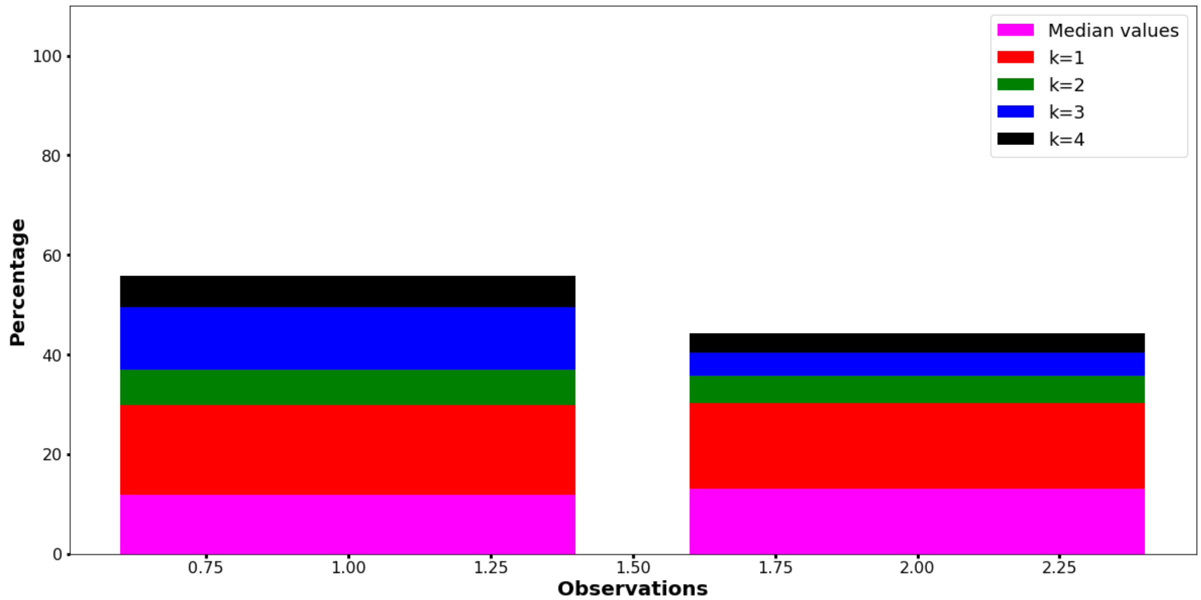

Uncertainty

	Num Datos (mean)	Num Datos (std)	Max. Distance Cluster (mean)	Max. Distance Cluster (std)
Min.Rot. Angle > 30º	11.27	6.62	70.02	30.08

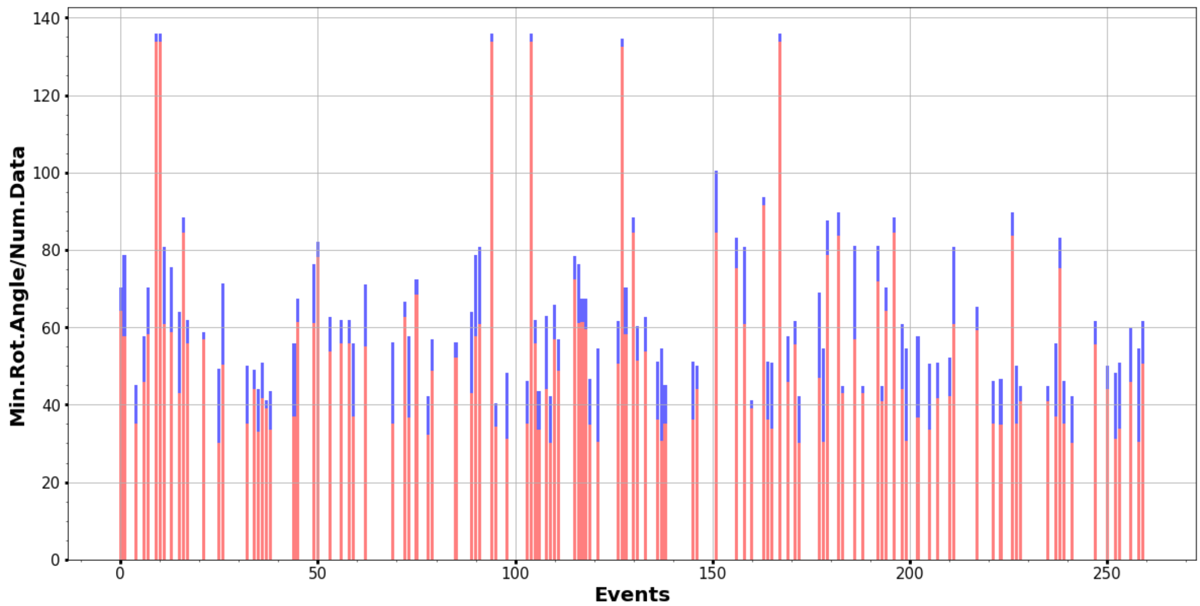

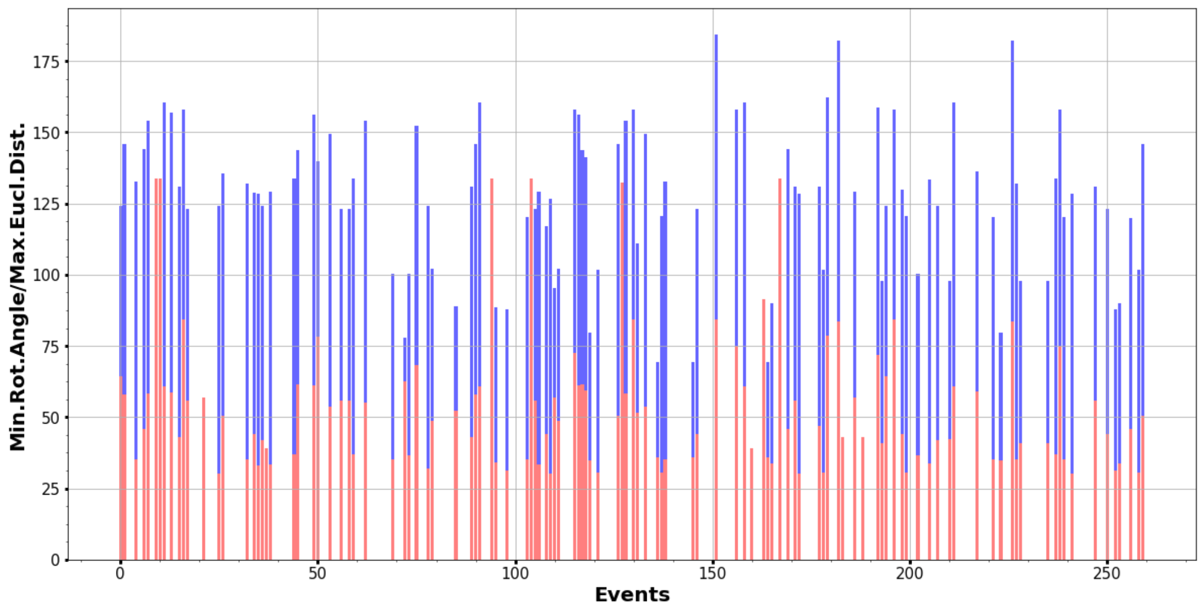

	Num Datos (mean)	Num Datos (std)	Max. Distance Cluster (mean)	Max. Distance Cluster (std)
Min.Rot. Angle <= 30º	15.48	6.68	69.14	22.27

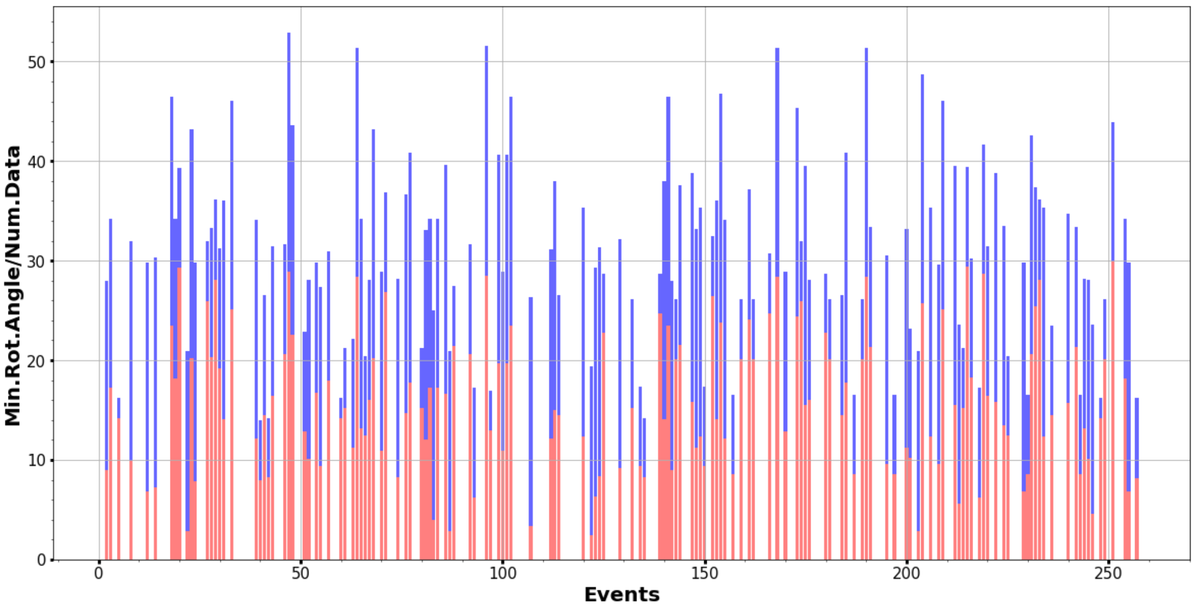
Min.Rot.Angle/Num.Data
Events

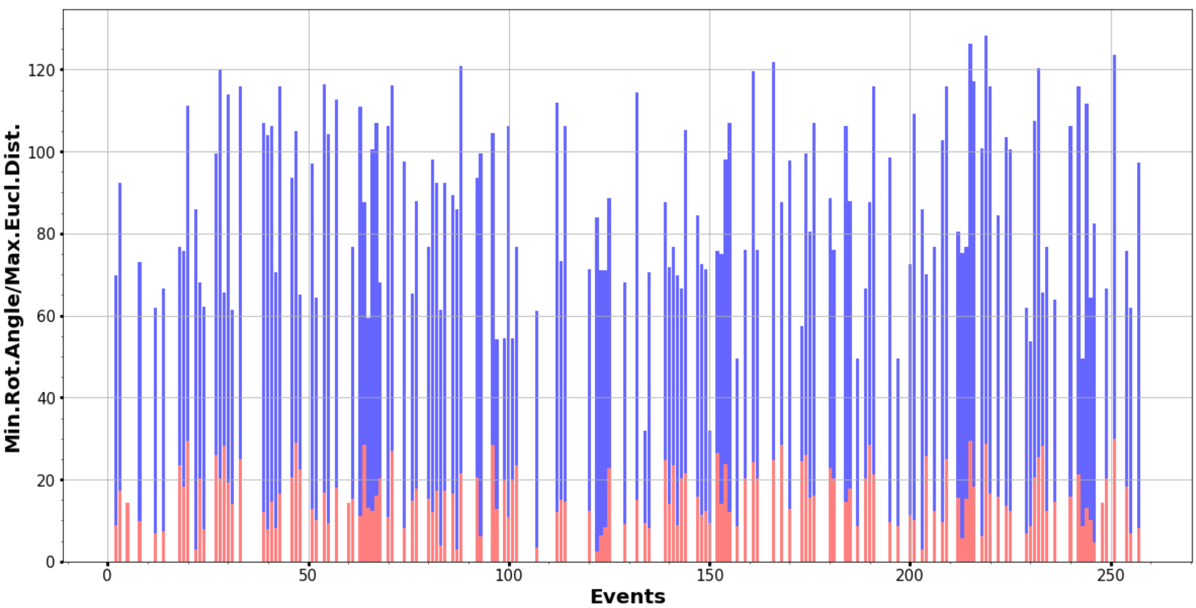
Min.Rot.Angle/Max.Eucl.Dist.
Events

Minimum Rotated Angle Results (including fault geometry)

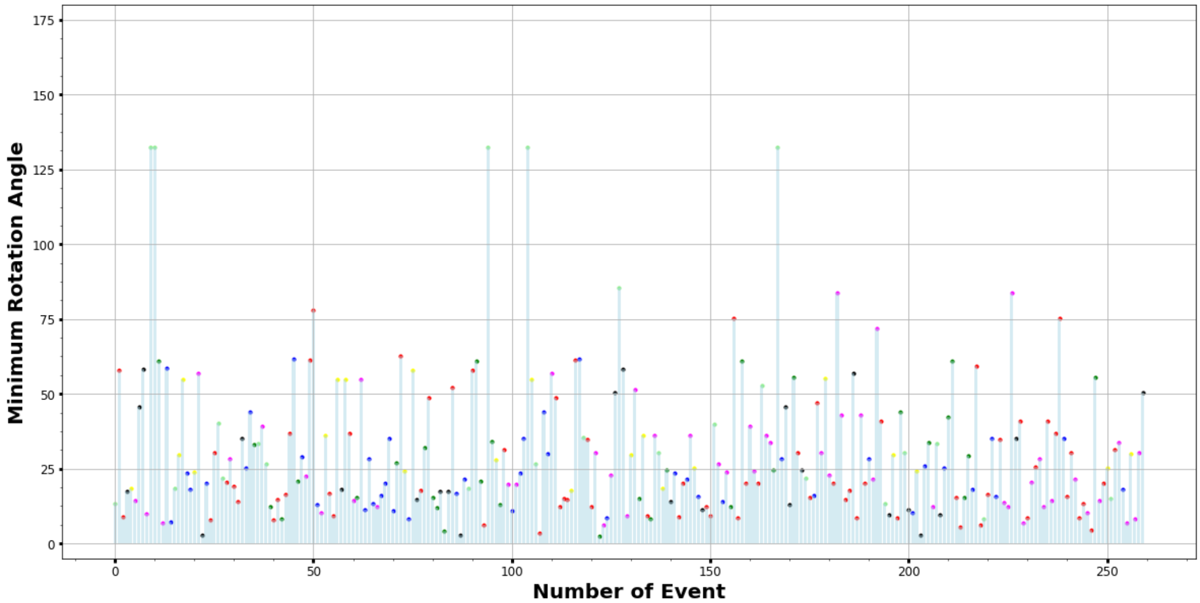

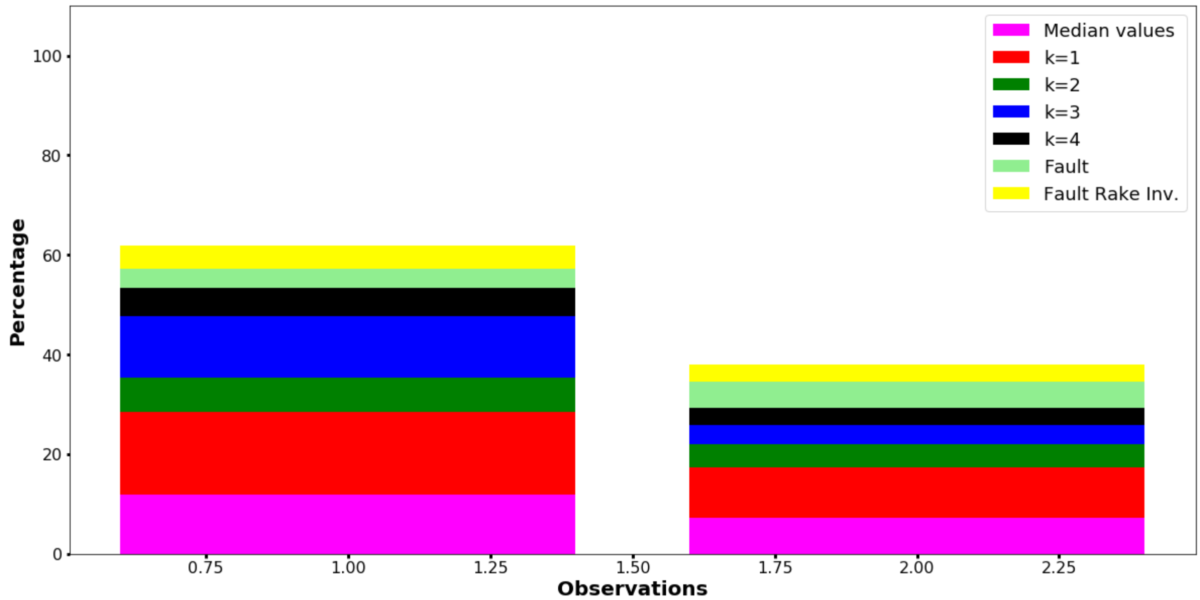

Seed 91

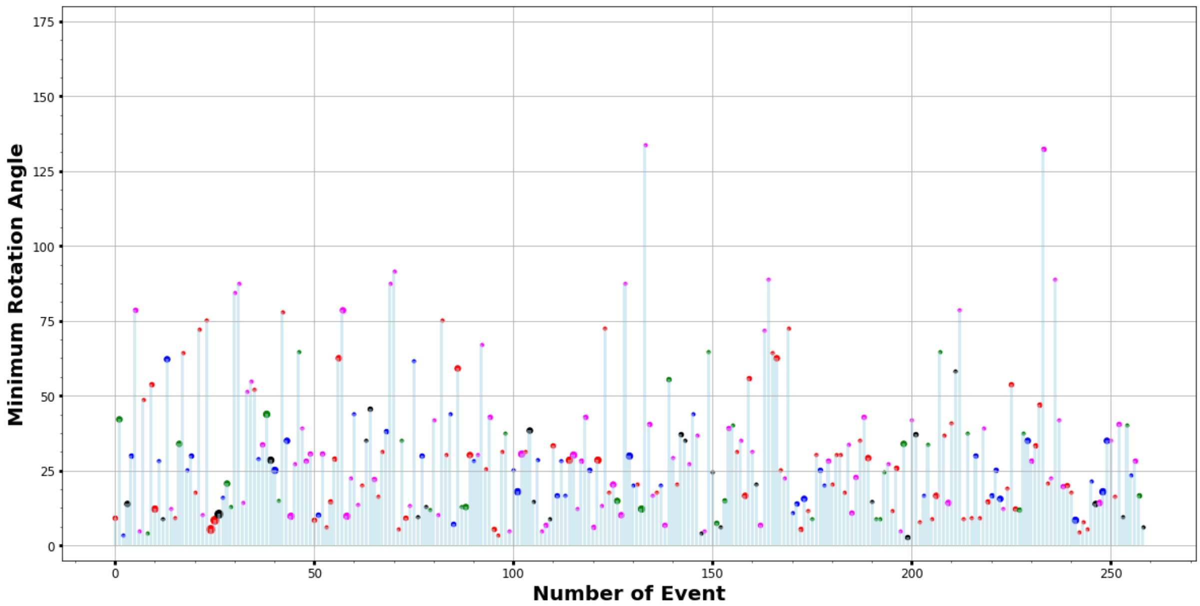

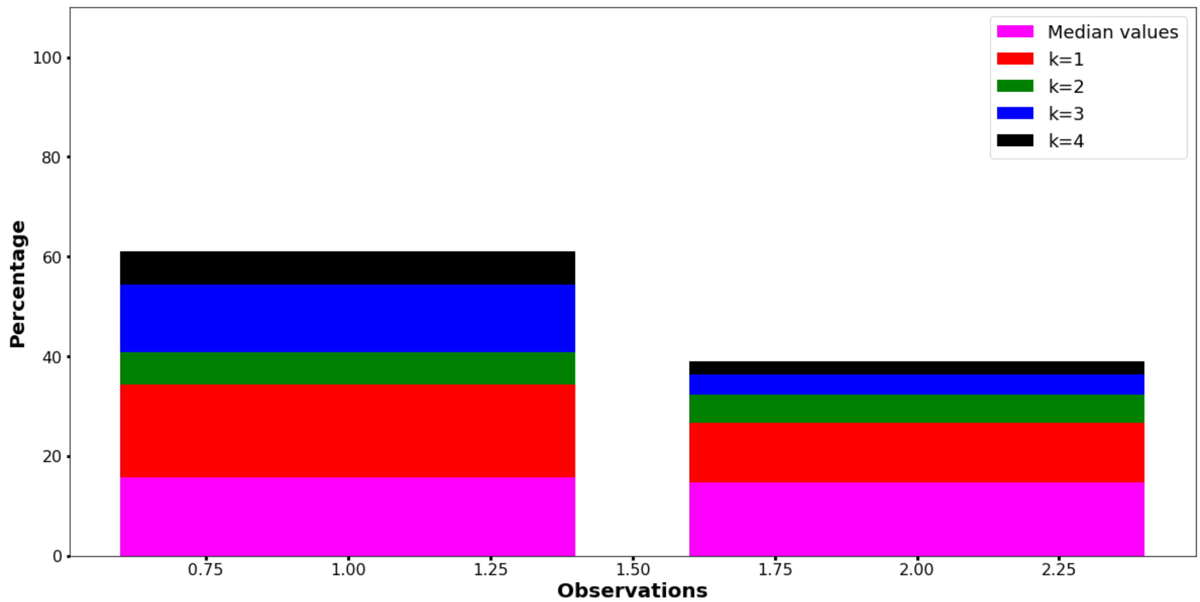

Uncertainty

	Num Datos (mean)	Num Datos (std)	Max. Distance Cluster (mean)	Max. Distance Cluster (std)
Min.Rot. Angle > 30º	11.15	6.54	63.19	27.78

	Num Datos (mean)	Num Datos (std)	Max. Distance Cluster (mean)	Max. Distance Cluster (std)
Min.Rot. Angle <= 30º	15.48	6.68	68.78	28.32

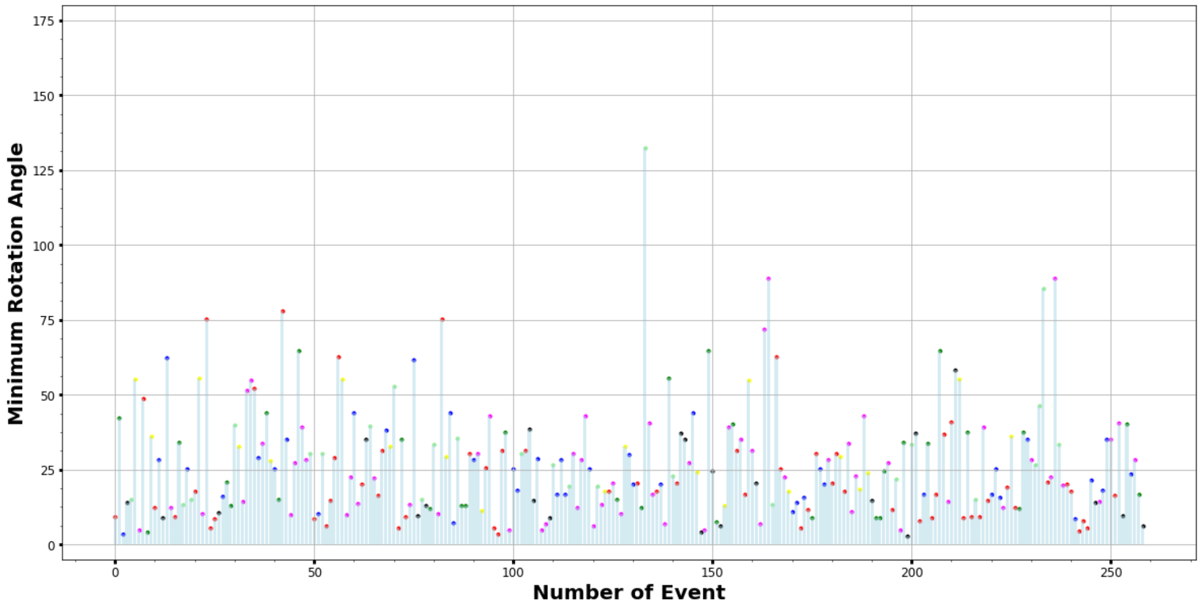

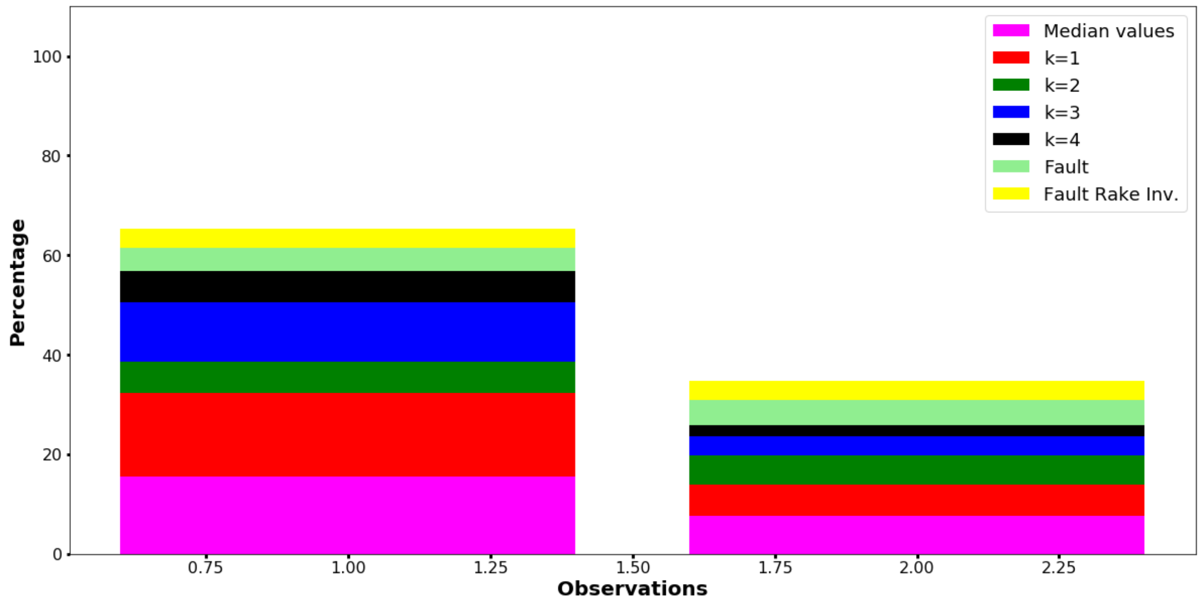

Results over random selection events: 273 approx.

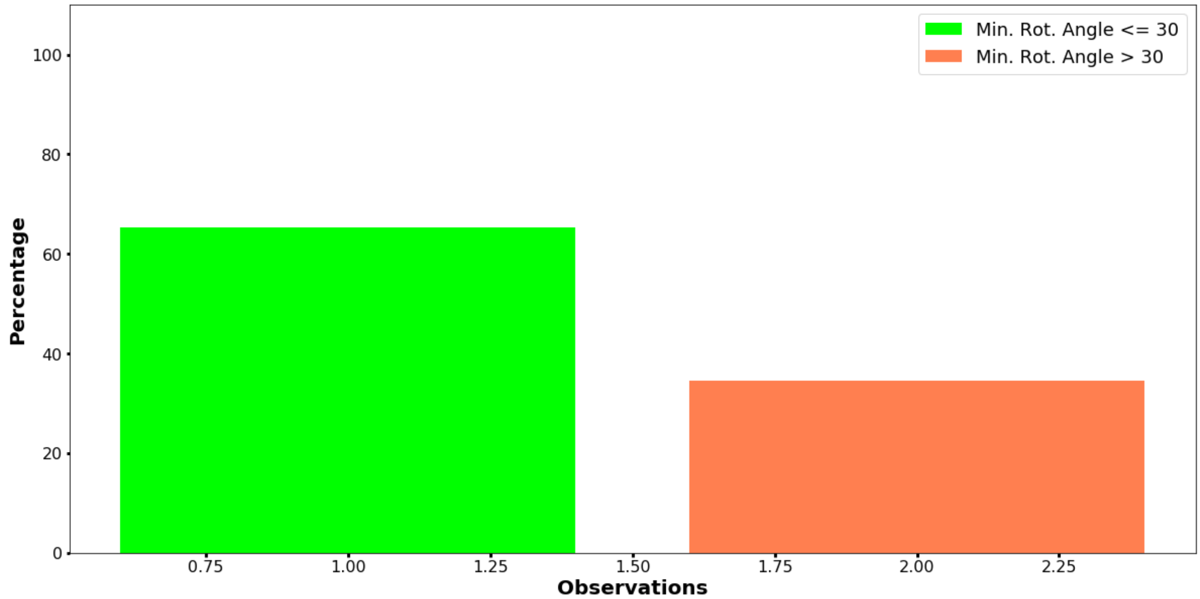

Fig. 14 Statistical results of MRA analysis. Percentage of similar focal mechanism shown in green, and non-similar focal mechanism in orange.

3.4 Study case : Southern California

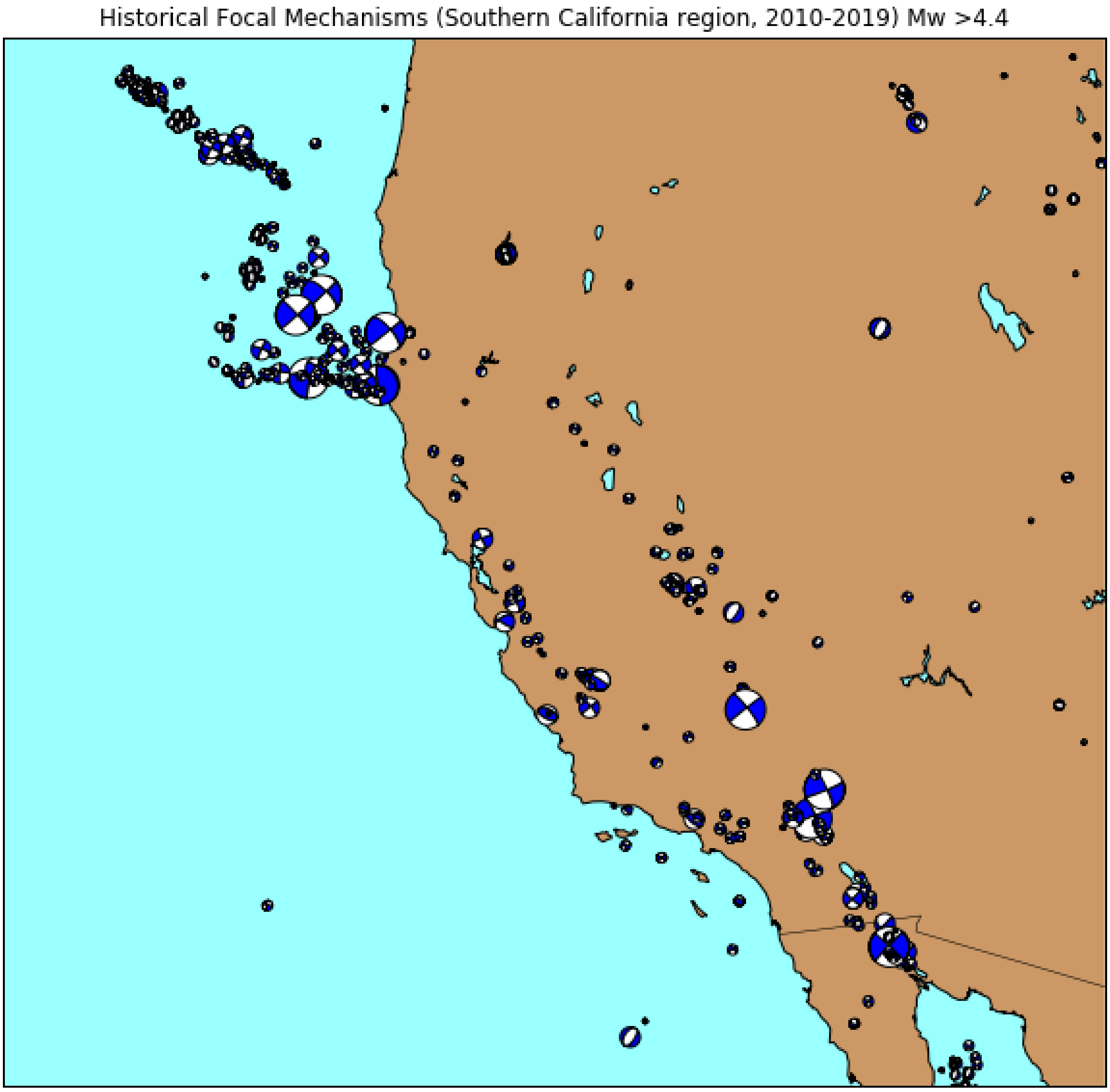

Fig. 15 California region and focal mechanisms database for M>4.4

Exploratory analysis

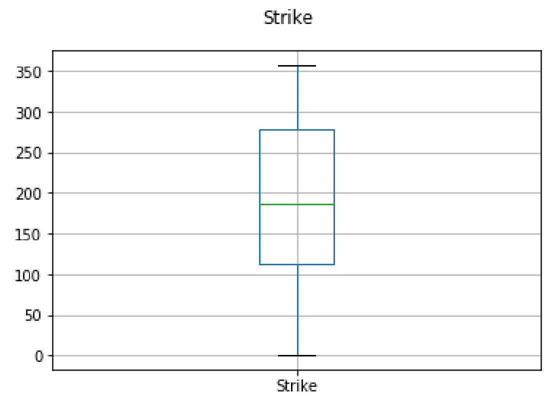

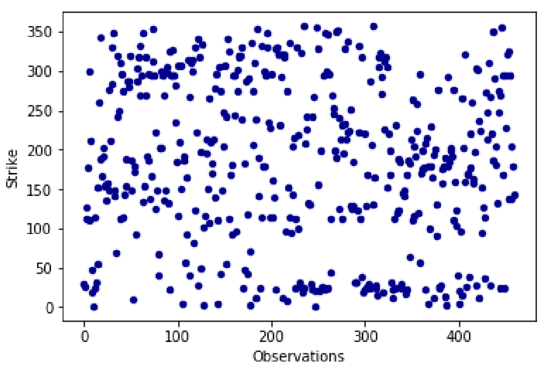

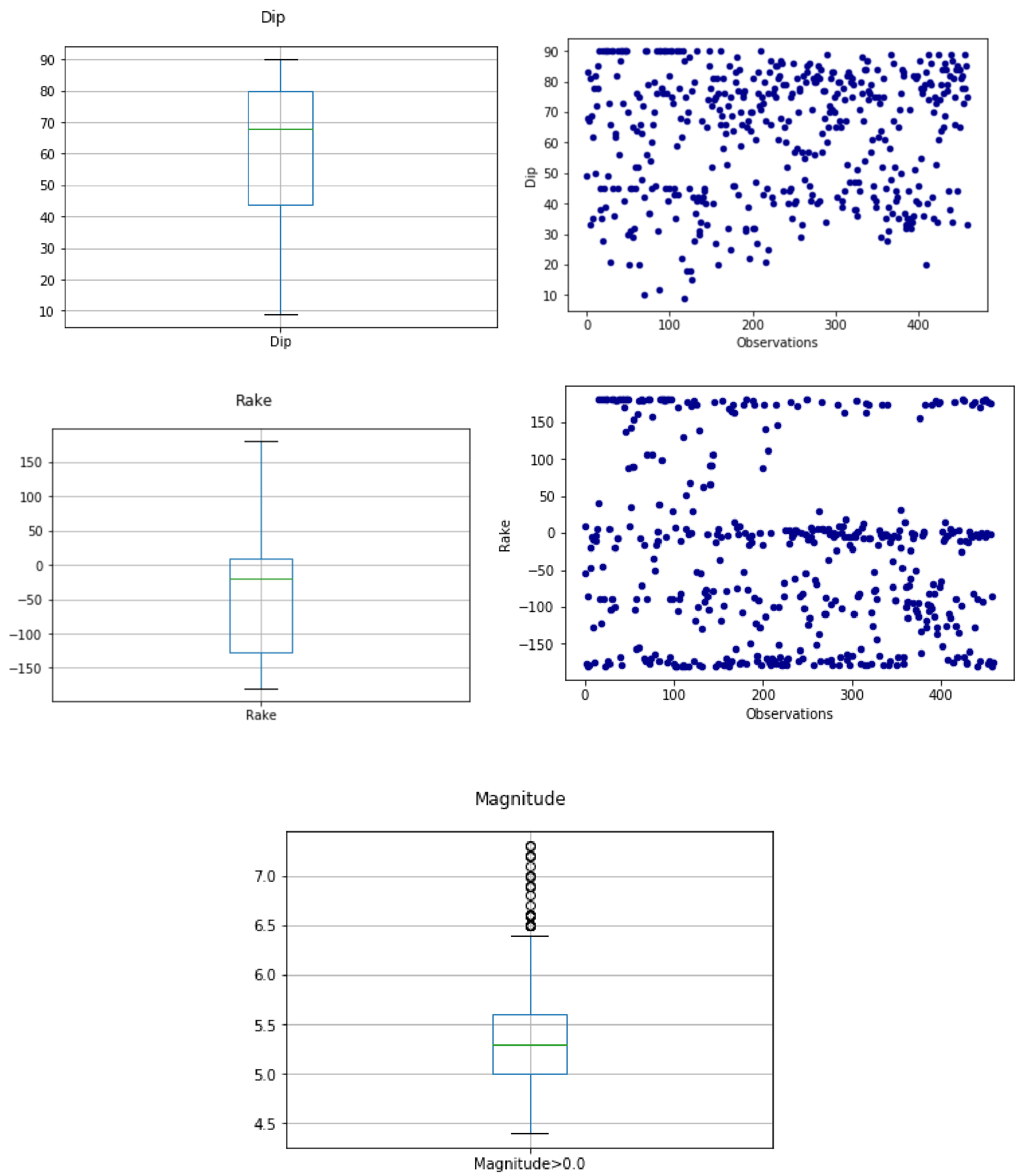

Fig. 16 Statistical distribution of strike, dip, rake and magnitude for California database

Parameters

k = 20 # Number of neighbors
Dist_th = 100 # Maximum distance threshold [km]
Mag_th = 4.4 # Minimum magnitude threshold
Seed = 98

Minimum Rotated Angle Results

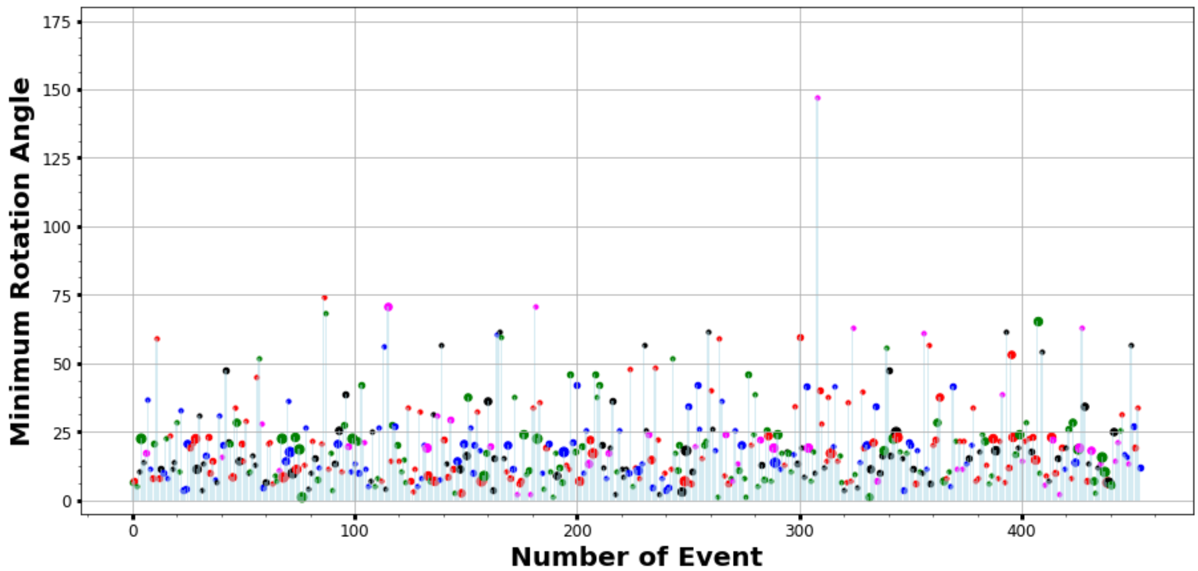

Fig. 17 MRA results combining the best values from k=1, 2, 3, 4 and the median hypothetical focal mechanism

Results over random selection events: 450 approx

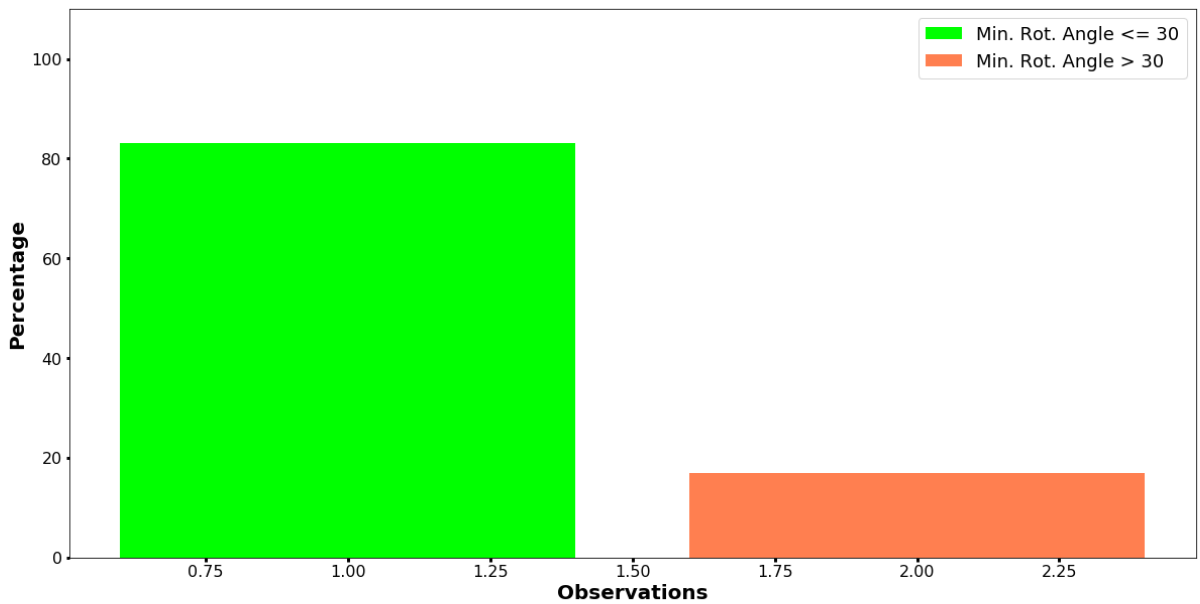

Fig. 18 Statistical results of MRA analysis. Percentage of similar focal mechanism shown in green, and non-similar focal mechanism in orange.

3.5 Study case : Italy

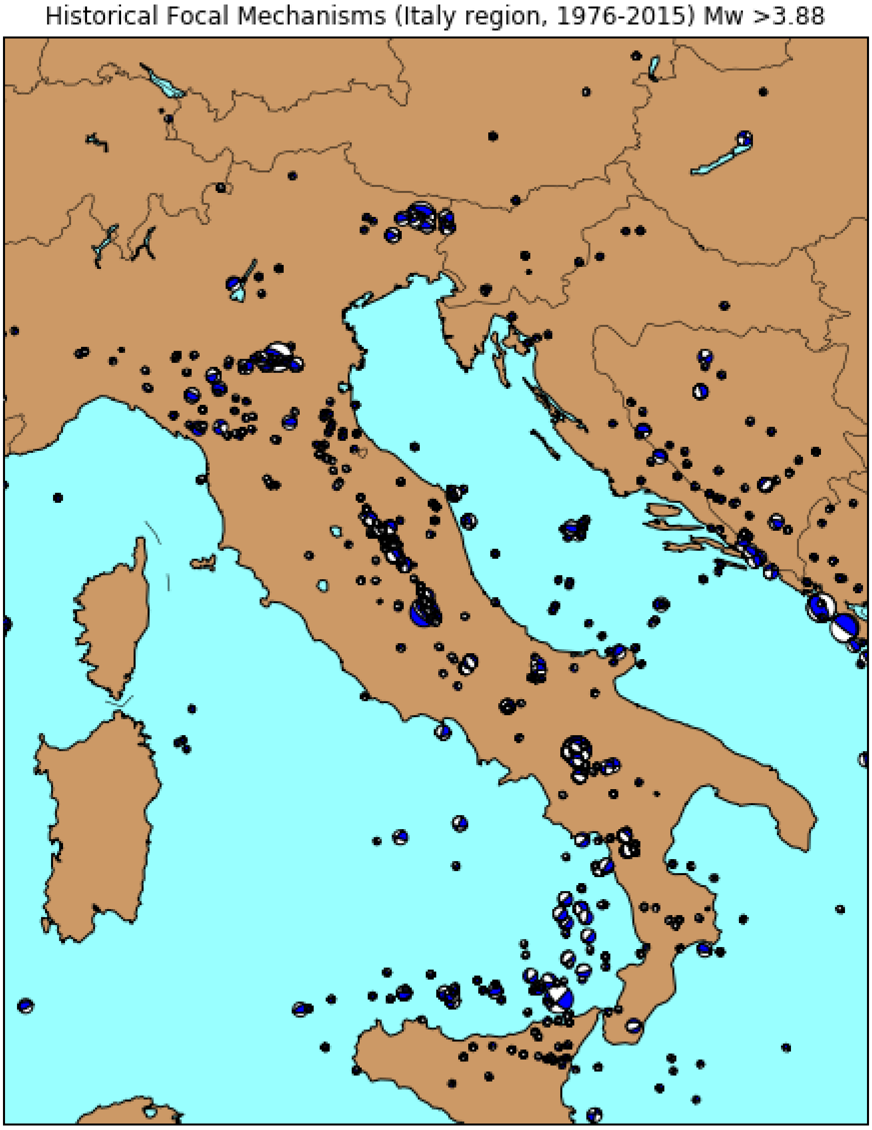

Fig. 19 The Italian region and focal mechanisms database for M>3.88

Exploratory analysis

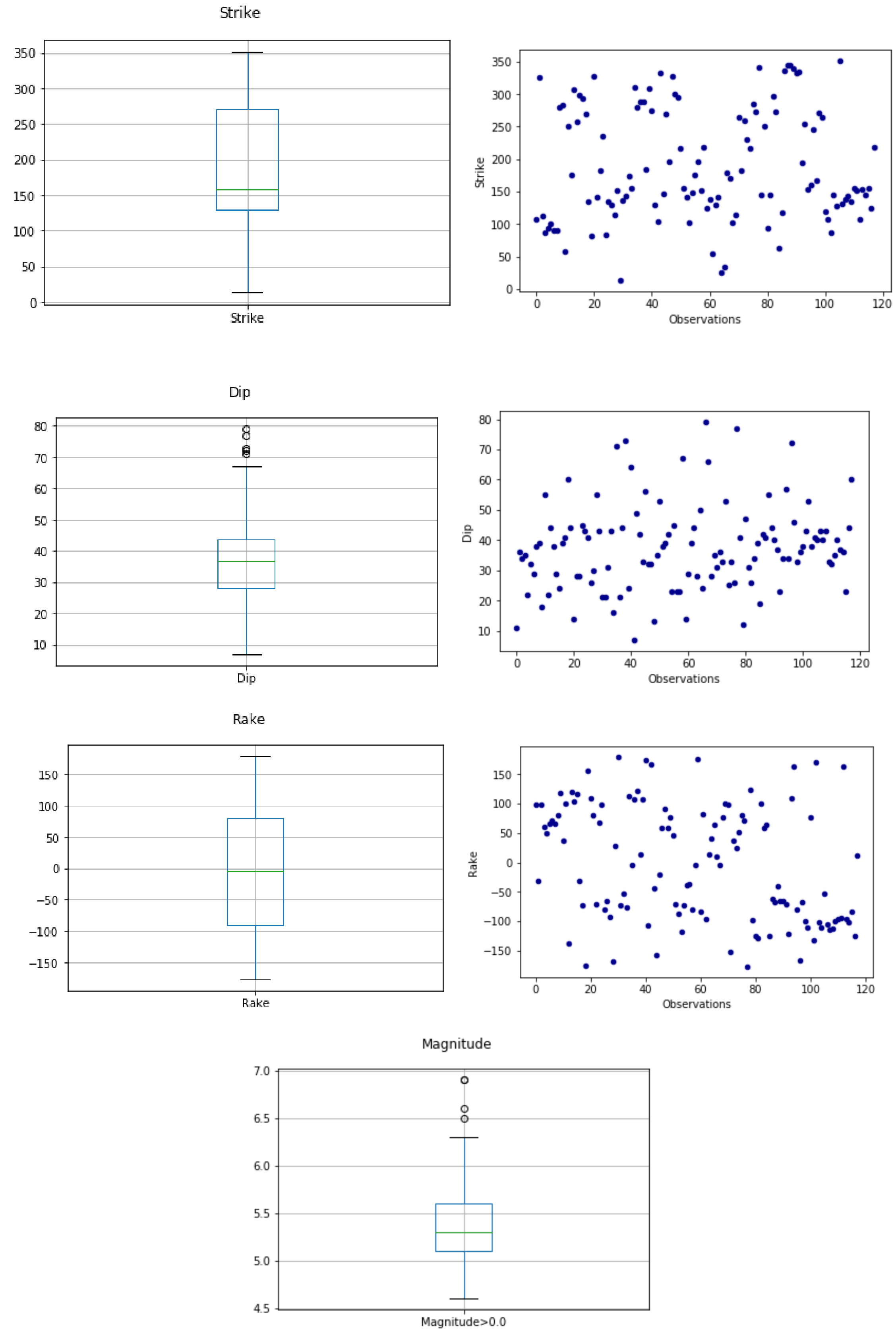

Fig. 20 Statistical distribution of strike, dip, rake and magnitude for the Italian database

Parameters

k = 20 # Number of neighbors
Dist_th = 100 # Maximum distance threshold [km]
Mag_th = 3.9 # Minimum magnitude threshold
Seed = 98

Minimum Rotated Angle Results

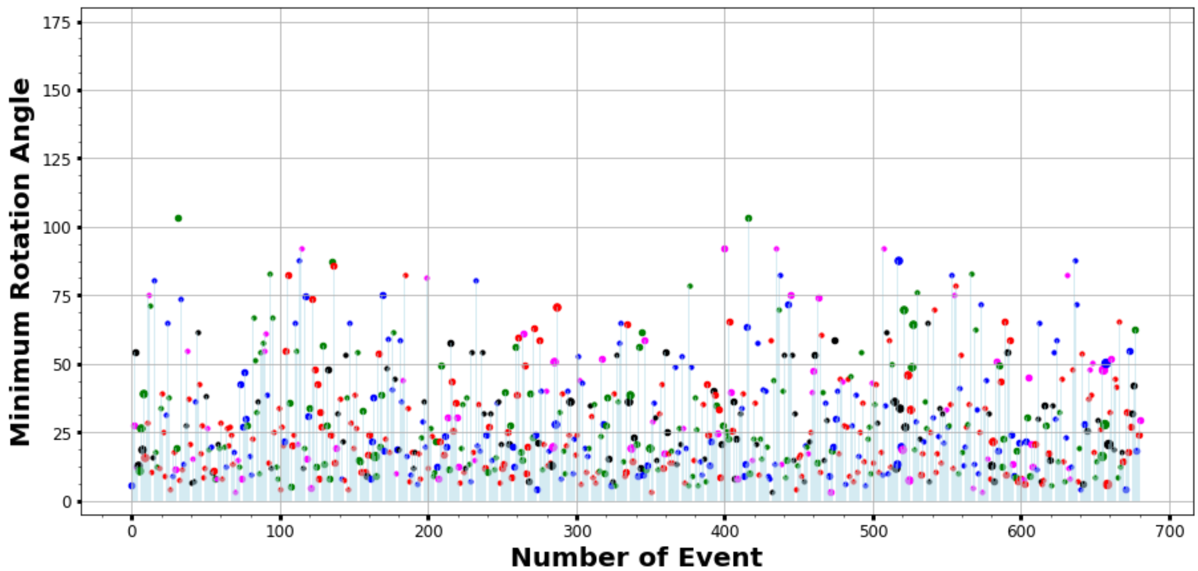

Fig. 21 MRA results combining the best values from k=1, 2, 3, 4 and the median hypothetical focal mechanism

Results over random selection events: 680 approx

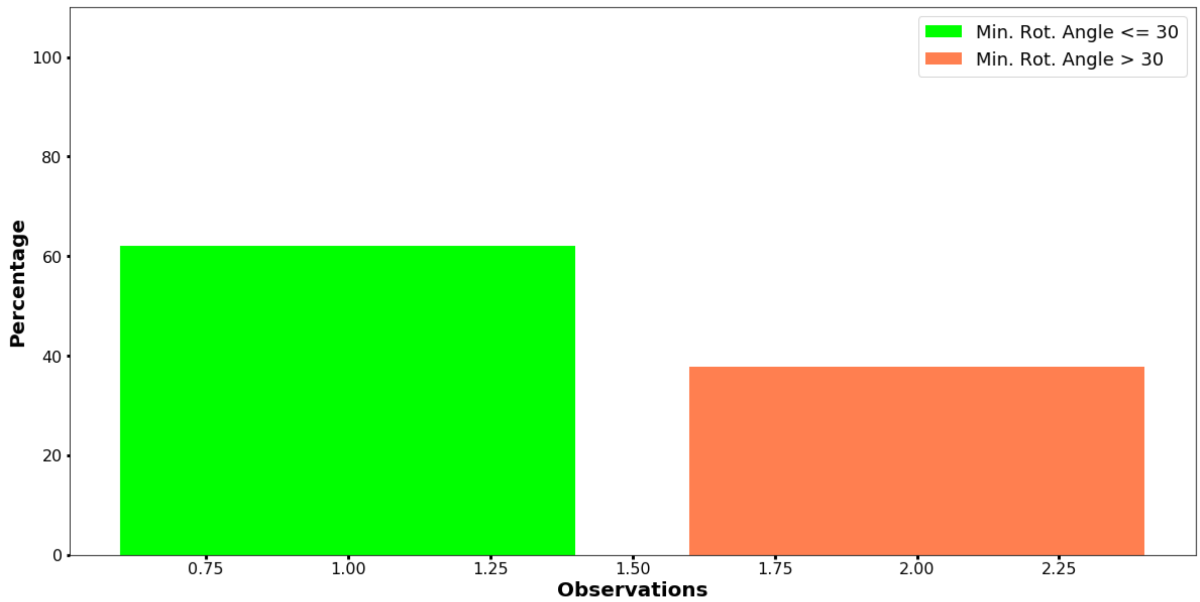

Fig. 22 Statistical results of MRA analysis. Percentage of similar focal mechanism shown in green, and non-similar focal mechanism in orange.

4. Discussion

After validate a large number of experiments we find that a value lower or equal of 30 degrees in the MRA measure gives a similar value than the real, while a MRA greater than 30 show a different values of focal mechanisms. When MRA is close to 90 the focal mechanisms shows an inverted faulting type, from normal to inverse (or vice versa). An example of these observations is shown in Fig. 3

The results shown that the lower MRA are not always provided by the closer event (k=1) or the median hypothetical. The similarity in the beach balls in some cases with other closer neighbors as k=2,3, or 4 also appears. Moreover, a explicit relation with the depth are not find (the plots are not included in this report).

The two regions with the better statistics are Japan and Southern California. Those study cases shown a 80% of probability to assign a similar focal mechanism for a new event. This could be related with two factors, the number of events and/or the similitude in the rupture type in these regions.

In the case of Italy, Iceland and New Zealand, the probability to assign a similar focal mechanism to a new event is around the 60%. However, as is mentioned before a large number in MRA not necessarily indicates a large difference between the focal mechanism of a new event and a past earthquakes. For example, a MRA close to 90 indicates an inversion in focal mechanism type (from normal to inverse).

5. Conclusion and Future work

In this research we develop a new tool to assign a focal mechanism to a new event. This tool uses historical CMT databases and a python code to find the better focal mechanism.

The probability of assign a similar value to the real depends on the region shows a region dependency. As a part of the PD1 workflow we will assign at least 5 CMT values including a uncertainty range for each angle (strike, dip, and rake). In future work we will include a sensibility analysis between the resulted time series obtained using different focal mechanisms. This analysis will give us a key for the better choosing the CMT that will be provided in the PD1 workflow.

References

Duputel, Z., Rivera, L., Kanamori, H., & Hayes, G. (2012). W phase source inversion for moderate to large earthquakes (1990–2010). *Geophysical Journal International*, *189*(2), 1125-1147.

Kagan, Y. Y. (2007). Simplified algorithms for calculating double-couple rotation. *Geophysical Journal International*, *171*(1), 411-418.

Lin, J. T., Chang, W. L., Melgar, D., Thomas, A., & Chiu, C. Y. (2019). Quick Determination of Earthquake Source Parameters from GPS Measurements: A Study of Suitability for Taiwan. *Geophysical Journal International*.

Maeda, N. (1992). A method of determining focal mechanisms and quantifying the uncertainty of the determined focal mechanisms for microearthquakes. *Bulletin of the Seismological Society of America*, *82*(6), 2410-2429.

Melgar, D., Bock, Y., & Crowell, B. W. (2012). Real-time centroid moment tensor determination for large earthquakes from local and regional displacement records. *Geophysical Journal International*, *188*(2), 703-718.

Okuda, T., & Ide, S. (2018). Hierarchical rupture growth evidenced by the initial seismic waveforms. *Nature communications*, *9*(1), 3714.

Sinnott, R. W. (1984). Virtues of the Haversine. *Sky Telesc.*, *68*, 159.

Tarantino, S., Colombelli, S., Emolo, A., & Zollo, A. (2019). Quick Determination of the Earthquake Focal Mechanism from the Azimuthal Variation of the Initial P-Wave Amplitude. *Seismological Research Letters*.